UNIVERSIDADE ESTADUAL DE MARINGÁ

CENTRO DE CIÊNCIAS BIOLÓGICAS

PROGRAMA DE PÓS-GRADUAÇÃO EM CIÊNCIAS BIOLÓGICAS

ÁREA DE CONCENTRAÇÃO EM BIOLOGIA CELULAR E MOLECULAR

FABIANNE MARTINS RIBEIRO

ESTUDO DO MECANISMO FOTOPROTETOR DE DIFERENTES ABORDAGENS TERAPÊUTICAS SOBRE DANO OXIDATIVO INDUZIDO POR RADIAÇÃO ULTRAVIOLETA A e B

Maringá

2019

FABIANNE MARTINS RIBEIRO

ESTUDO DO MECANISMO FOTOPROTETOR DE DIFERENTES ABORDAGENS TERAPÊUTICAS SOBRE DANO OXIDATIVO INDUZIDO POR RADIAÇÃO ULTRAVIOLETA A e B

Tese apresentada ao Programa de Pós-Graduação em Ciências Biológicas (área de concentração - Biologia Celular e Molecular), da Universidade Estadual de Maringá para a obtenção do grau de Doutor em Ciências Biológicas.

Orientador: Prof. Dr. Celso Vataru Nakamura

Maringá

2019

Dados Internacionais de Catalogação-na-Publicação (CIP)
(Biblioteca Central - UEM, Maringá - PR, Brasil)

R484e

Ribeiro, Fabianne Martins
Estudo do mecanismo fotoprotetor de diferentes abordagens terapêuticas sobre dano oxidativo induzido por radiação ultravioleta A e B / Fabianne Martins Ribeiro. -- Maringá, PR, 2019.
68 f.: il. color.

Orientador: Prof. Dr. Celso Vataru Nakamura.
Tese (Doutorado) - Universidade Estadual de Maringá, Centro de Ciências Biológicas, Departamento de Biotecnologia, Genetica e Biologia Celular, Programa de Pós-Graduação em Ciências Biológicas (Biologia Celular), 2019.

1. Fotoenvelhecimento. 2. Raios ultravioleta. 3. Estresse oxidativo. 4. Antioxidantes. I. Nakamura, Celso Vataru, orient. II. Universidade Estadual de Maringá. Centro de Ciências Biológicas. Departamento de Biotecnologia, Genetica e Biologia Celular. Programa de Pós-Graduação em Ciências Biológicas (Biologia Celular). III. Título.

CDD 23.ed. 616.5

Márcia Regina Paiva de Brito - CRB-9/1267

FABIANNE MARTINS RIBEIRO

ESTUDO DO MECANISMO FOTOPROTETOR DE DIFERENTES ABORDAGENS TERAPÊUTICAS SOBRE DANO OXIDATIVO INDUZIDO POR RADIAÇÃO ULTRAVIOLETA A e B

Tese apresentada ao Programa de Pós-Graduação em Ciências Biológicas (área de concentração - Biologia Celular e Molecular), da Universidade Estadual de Maringá para a obtenção do grau de Doutor em Ciências Biológicas.

Aprovado em: 09/12/2019

BANCA EXAMINADORA*

_____

Prof. Dr. Celso Vataru Nakamura
Universidade Estadual de Maringá

_____

Profa. Dra. Rúbia Casagrande
Universidade Estadual de Londrina

_____

Profa. Dra. Anacharis Babeto de Sá Nakanishi
Universidade Estadual de Maringá

_____

Profa. Dra. Karin Juliane Pelizzaro Rocha Brito
Centro Universitário Cesumar

_____

Prof. Dr. Jean Henrique da Silva Rodrigues
Universidade Federal da Integração Latino-Americana

BIOGRAFIA

Fabianne Martins Ribeiro nasceu em Rio Verde/GO em 2 de fevereiro de 1984. Possui graduação em Ciências Biológicas (Licenciatura) pela Universidade Federal de Mato Grosso (2007) campus Primavera do Leste, MT, e em Farmácia pela Universidade de Rio Verde (2011), campus Rio Verde, Goiás. Durante a graduação realizou pesquisa envolvendo a química analítica de titulações por oxi/redução e suas aplicações. Possui mestrado em Ciências Farmacêuticas (PCF) pela Universidade Estadual de Maringá. Dedicou-se desde o início do mestrado (2013) no estudo do potencial fotoquimioprotetor de compostos antioxidantes, utilizando radiação ultravioleta A e B, bem como o possível mecanismo de ação, sob orientação da Profa. Dra. Sueli de Oliveira Silva Lautenschaler e Prof. Dr. Celso Vataru Nakamura.

APRESENTAÇÃO

Esta tese é composta por dois artigos científicos contemplando os resultados obtidos durante o curso de doutorado. Em consonância com as regras do Programa de Pós-Graduação em Ciências Biológicas, ambos os artigos foram escritos e, posteriormente serão publicados em periódicos que atenda aos critérios vigentes estabelecidos pela CAPES.

O primeiro artigo relata os resultados contidos no artigo intitulado "Metformin effect on driving cell survival pathway through inhibition of UVB-induced ROS formation in human keratinocytes", que descreve a atividade biológica e o possível mecanismo de ação de um composto natural sobre cultura de células submetidas a danos induzidos pela radiação ultravioleta B.

O segundo artigo relata os resultados contidos no artigo intitulado "Effect of cerium oxide nanoparticles on fibroblasts L929 proliferation, aging and death: Further studies on protective mechanisms against UVA-induced damage", que descreve outra abordagem terapêutica, constituído pelo estudo do possível mecanismo de ação de um composto sintético em cultura de células submetidas a danos induzidos pela radiação ultravioleta A.

AGRADECIMENTOS

Á minha família, meus pais Antônio e Suely, aos meus sogros Nivaldo e Nadir, e em especial ao meu esposo Fabiano, pela paciência e compreensão, que forneceram continuamente seu apoio moral, espiritual, emocional. Obrigada pela compreensão da nossa ausência nesse período.

Ao meu orientador Celso Nakamura pela confiança depositada, por ter abrido as portas do seu laboratório, fazendo-me compreender cada etapa com mais maturidade. Por todo o seu conhecimento científico, por nos ensinar a "persistir no esforço", exemplo de ética a ser seguido, sempre mostrando a todos como ser grande com humildade. Obrigada por ensinar que com muito trabalho, disposição e perseverança é possível alcançar os objetivos.

Às professoras Tânia Ueda Nakamura e Sueli Lautenschlager pelo apoio técnico, pela fonte de inspiração e ensinamentos para o meu crescimento pessoal e profissional. Em especial à Professora Sueli, obrigada por sua amizade, compreensão, pelo seu tempo sempre disponibilizado (incluindo às noites de trabalho), pela credibilidade e paciência que foram imprescindíveis para a minha "caminhada científica". Muito obrigada pelo exemplo!

Aos colegas do laboratório "B-08" que se tornaram minha família ao longo desses anos. Todos contribuíram de alguma forma para a realização deste trabalho e para o meu crescimento. Em especial à Mariana Maciel de Oliveira, pela disponibilidade e ajuda foi muito importante na fase final. Aos amigos Hélito Volpato, Danielle Bidóia, Fabiana Rando, Jean Henrique, Bianca Ratti, Karina Miyuki, Érica Zanqueta, que compartilharam suas palavras de conselho e incentivo para concluir este estudo.

Aos técnicos do Complexo de Centrais de Apoio à Pesquisa (COMCAP/UEM) pelo apoio na execução dos experimentos.

À secretaria de pós-graduação em Ciências Biológicas (PBC), em especial ao Nelsino e à Érica, por sempre procurar ajudar-me em toda a parte burocrática.

Às instituições que financiaram o trabalho de pesquisa, Conselho Nacional de Desenvolvimento Científico e Tecnológico (CNPq), Fundação Araucária e à Coordenação de Aperfeiçoamento de Pessoal de Nível Superior (CAPES) pela bolsa de estudos concedida.

RESUMO GERAL

1. Introdução

A pele humana funciona como uma barreira de proteção e mantém a homeostase. A exposição à radiação ultravioleta (UV) é responsável pelo envelhecimento prematuro da pele e pela carcinogênese, causada principalmente pela superprodução de espécies reativas de oxigênio (ERO). Há um interesse crescente por pesquisas sobre novas estratégias que abordem a prevenção do fotoenvelhecimento.

Avaliamos o potencial da metformina em proteger as células de queratinócitos HaCaT dos danos causados pela radiação UVB, bem como seu possível mecanismo de ação. Observamos que a metformina não mostrou atividade antioxidante intrínseca, mas foi capaz de reduzir a produção de ERO intracelular induzida por UVB e superóxido ($O_2^{\bullet-}$) dependente de NADPH oxidase. Além disso, reduziu a fosforilação de ERK 1/2, a atividade da NADPH oxidase e morte celular por apoptose. Esses resultados mostraram que este estudo traz evidências de que a metformina pode ser um promissor agente antienvelhecimento contra danos à pele induzidos pela radiação UVB. No outro estudo, fibroblastos L929 foram tratadas com nanoceria (100 nM) e expostas à radiação UVA. O pré-tratamento de células com nanoceria não mostrou citotoxicidade e protegeu as células da morte induzida por UVA, aumentando a viabilidade celular. Nanoceria também diminuiu a produção de ERO imediatamente após a irradiação ou por até 48 horas e ainda restaurou a atividade de SOD e GSH. Além disso, o tratamento com nanoceria impediu a apoptose, diminuindo os níveis de Caspase 3/7 e a perda de potencial da membrana mitocondrial. Nanoceria também aumentou significativamente a sobrevivência celular, aumentando a proliferação por 5 dias em comparação com as células não irradiadas e nas células irradiadas por UVA e no ensaio de cicatrização de feridas. Além disso, verificou-se que a nanoceria diminuiu o envelhecimento celular e a fosforilação de ERK 1/2. Nosso estudo sugere que a nanoceria pode ser um potencial aliado das enzimas antioxidantes intracelulares para combater a foto-lesão induzida por UVA e, consequentemente, levar as células a mecanismos de sobrevivência e proliferação. Assim, nosso objetivo foi avaliar a atividade biológica e o mecanismo de ação de duas abordagens de tratamento em danos induzidos por radiação UV em modelos de cultura de células.

Palavras-chave: nanopartícluas de óxido de cério, antioxidantes, metformina, radiação ultravioleta

2. Metodologias

Os ensaios de atividade biológica e elucidação dos mecanismos de ação foram realizados com culturas de células de queratinócitos humanos da linhagem HaCaT e fibroblastos murinos L929.

As células HaCaT foram tratadas com metformina e submetidas à radiação ultravioleta B. A metformina foi adquirida comercialmente da Sigma Aldrich (PHR1084).

As células L929 foram tratadas com nanopartículas de óxido de cério (nanoceria) e submetidas à radiação ultravioleta A. As nanopartículas de óxido de cério foram sintetizadas pelo grupo de pesquisa do Prof. Dr. Sudipta Seal da Universidade Central da Flórida (University of Central Florida, UCF, Orlando, USA).

2.1 Atividade biológica da metformina sobre queratinócitos HaCaT irradiados com UVB

Com o objetivo de verificar o possível mecanismo de ação fotoprotetor e um possível envolvimento de atividade antioxidante, as células foram tratadas com 1 μM de metformina, irradiadas com UVB (40 mJ/cm^2) e processadas para os ensaios: citotxicidade e fotoproteção (MTT); ensaio do DPPH•, Xantina oxidase (XOD); produção de espécies reativas de oxigênio (H_2DCF-DA), atividade da enzima NADPH oxidase; morte celular por apoptose (Anexina V/PI), fosoforilação da proteína ERK 1/2 por Western blot.

2.2 Atividade biológica das nanopartículas de óxido de cério sobre fibroblastos L929 irradiados com UVA

Com o objetivo de verificar o possível mecanismo de ação fotoprotetor, as células foram tratadas com 100 nM de nanoceria, irradiadas com UVA (30 J/cm^2) e processadas para os ensaios: citotoxicidade e fotoproteção (MTT); produção de espécies reativas de oxigênio (H_2DCF-DA), atividade das enzimas intracelulares superóxido dismutase (SOD) e glutationa (GSH); ensaio de proliferação e cicatrização de ferida; envelhecimento (β-galactosidase) e morte celular por apoptose (nível de Caspases 3/7, potencial de membrana mitocondrial), envolvimento da via de sobrevivência MAPK ERK 1/2 (Western blot).

3. Resultados e discussão

3.1 Atividade fotoprotetora da metformina sobre queratinócitos HaCaT irradiados com UVB

A metformina demonstrou evidências de sua atividade fotoprotetora na concentração de 1 μM. Utilizando metodologias para elucidação do mecanismo de ação, verificamos importantes danos celulares induzidos pela radiação UVB, como o aumento dos níveis de espécies reativas de oxigênio (ERO), ativação da enzima NADPH oxidase, morte celular por apoptose e aumento da fosforilação da proteína ERK 1/2.

Em relação à atividade antioxidante, a metformina dimimuiu os níveis de ERO. Curiosamente, verificamos que a metformina não apresentou atividade antioxidante intrínseca na concentração testada, mas sim agindo indiretamente sobre potenciais fontes de ERO, como a enzima NADPH oxidase, que é também responsável pela produção extendida de ERO após a irradiação. A produção extendida de ERO pode levar à ativação de vias que controlam a sobrevivência e morte celular, como a MAPK ERK 1/2.

Estes resultados mostram evidências que podem servir como base para nossos estudos, de que a metformina pode ser uma nova abordagem para o tratamento de danos na pele causados pela radiação UVB.

3.2 Atividade fotoprotetora de nanopartículas de óxido de cério sobre fibroblastos L929 irradiados com UVA

Nanoceria apresentou atividade antioxidante ao dimimuir os níveis de ERO e restaurar a atividade de enzimas intracelulares (SOD e GSH). Porém, também foi observado um aumento da proliferação celular, cicatrização de ferida, diminuição da morte celular por apoptose, diminuição da senescência e diminuição da fosforilação da MAPK ERK 1/2.

Estes resultados mostram que além da atividade antioxidante, que já está bem estababelecida na literatura, o seu potencial regenerador pode ser explorado frente a danos causados pela radiação UVA.

4. CONCLUSÕES E PERSPECTIVAS

Os resultados obtidos neste trabalho trata-se de duas abordagens terapêuticas com diferentes mecanismos de ação em modelo de culturas de células da pele sob o dano induzido pela radiação ultravioleta A e B.

Ambos não apresentaram potencial citotóxico nas células testadas, sendo que nanoceria ainda induziu a proliferação celular. Além disso, ambos apresentaram atividade antioxidante por diferentes mecanismos;

Utilizando ensaios de mecanismo de ação, verificamos que a metformina e nanoceria reduziram os danos celulares oxidativos induzidos por UVA e UVB, que podem estar relacionados à morte celular por apoptose;

Desta forma, é possível concluir que a metformina e nanoceria apresentaram uma promissora atividade fotoprotetora por diferentes mecanismos de ação, trazendo novas abordagens terapêuticas e servindo como base para outros estudos que envolvem sua aplicação no tratamento dos danos causados pela radiação ultravioleta.

ABSTRACT

1. Introduction

Human skin works as a barrier of protection and maintains skin homeostasis. Exposure to ultraviolet radiation (UV) is responsible for premature skin aging and carcinogenesis mainly driven by overproduction of reactive oxygen species (ROS). There is a growing interest for research on new strategies that address the photoaging prevention.

We evaluate metformin potential on protect HaCaT keratinocytes cells from UVB irradiation induced damage as well as it possible mechanism of action. We observed that metformin did not show intrinsic scavenging activity but was able to reduce UVB-induced intracellular ROS and NADPH oxidase-dependent superoxide ($O_2^{\bullet-}$) production. Furthermore, reduced ERK 1/2 phosphorylation, NADPH oxidase activity and cell death by apoptosis. These results showed that MET might be a promising anti-photoaging agent against UV radiation induced skin damage.

In the other study, fibroblasts cells L929 were treated with nanoceria (100 nM) and exposed to UVA radiation and assayed for cell viabilty, oxidative stress by evaluation of ROS production, SOD and GSH activity and cell death and proliferation. Pretreatment of cells with nanoceria showed no cytotoxicity and protected cells from UVA-induced death by increasing of cell viability. Nanoceria also decreased ROS production imediately after irradiation or for up to 48h and restored SOD and GSH activity. Additionally, nanoceria treatment prevented apoptosis by decreasing Caspase 3/7 levels and mitochondrial membrane potential loss. Nanoceria significantly improved cell survival by increasing of proliferation for 5 days compared with non-irradiated and in UVA-irradiated cells and in wound healing assay. Furthermore, it was found that nanoceria decreased cell aging and ERK 1/2 phosphorylation. Our study suggests that nanoceria might be a potential ally with the intracellular antioxidant enzymes to fight UVA-induced photodamage and consequently drive cells to survival and proliferate mechanisms.

Thus, our objective was to evaluate the biological activity and mechanism of action of two approaches of treatingin in UV radiation induced damage in cell culture models.

Keywords: cerium oxide nanoparticles, antioxidant, metformin, ultraviolet radiation

2. Methodologies

Biological activity and elucidation of mechanism of action assays were performed with HaCaT human keratinocyte and L929 murine fibroblastos cell cultures.

HaCaT cells were treated with metformin and subjected to UVB radiation. Metformin was purchased commercially from Sigma Aldrich (PHR1084).

The L929 cells were treated with cerium oxide nanoparticles (nanoceria) and subjected to UVA radiation. Cerium oxide nanoparticles were synthesized by research group of Prof. Dr. Sudipta Seal of the Central University of Florida (University of Central Florida, UCF, Orlando, USA).

2.1 Biological activity of metformin on UVB-irradiated HaCaT keratinocytes

In order to verify the possible mechanism of photoprotective action, HaCaT cells were treated with 1 μM of metformin, irradiated with UVB (40 mJ cm^2) and processed for the antioxidante activity, cytotoxicity and photoprotection assays: MTT method; DPPH assay, Xanthine oxidase system (XOD); production of reactive oxygen species (H_2DCF-DA), activity of NADPH oxidase enzyme; cell death (Annexin V/PI), ERK 1/2 protein phosphorylation by Western blot.

2.2 Biological activity of cerium oxide nanoparticles on UVA-irradiated L929 fibroblasts

In order to verify the possible mechanism of photoprotective action, L929 cells were treated with 100 nM nanoceria, irradiated with UVA (30 J/cm^2) and processed for the tests: cytotoxicity and photoprotection (MTT); production of reactive oxygen species (H_2DCF-DA), activity of intracellular superoxide dismutase (SOD) and glutathione (GSH) enzymes; proliferation and wound healing assay; aging (β-galactosidase activity) and cell death by apoptosis (Caspases level 3/7, mitochondrial membrane potential), involvement of the MAPK ERK 1/2 survival pathway (Western blot).

3. Results and discussion

3.1 Photoprotective effect of metformin on UVB-irradiated HaCaT keratinocytes

Metformin showed photoprotective activity at a concentration of 1μM. Using methodologies to elucidate the mechanism of action, we found important cellular

damage induced by UVB radiation, such as increased levels of reactive oxygen species (ROS), activation of NADPH oxidase enzyme, apoptosis cell death and increased ERK 1/2 protein phosphorylation.

Regarding antioxidant activity, metformin decreased ROS levels. Interestingly, we found that metformin showed no intrinsic antioxidant activity at the concentration tested, but rather indirectly acting on potential sources of ROS, such as the enzyme NADPH oxidase, which is also responsible for extended ROS production after irradiation. Extended production of ROS may lead to activation of pathways that control cell survival and death, such as MAPK ERK 1/2, that was reduced by metformin.

These results show evidence that may serve as the basis for our studies that metformin may be a new approach for treating skin damage caused by UVB radiation.

3.2 Photoprotective activity of cerium oxide nanoparticles on UVA-irradiated L929 fibroblasts

Nanoceria showed antioxidant activity by decreasing ROS levels and restoring the activity of intracellular enzymes (SOD and GSH). Moreover, increased cell proliferation, wound healing process, decreased apoptotic cell death and senescence, and decreased MAPK ERK 1/2 phosphorylation.

These results show that in addition to the antioxidant activity, which is already well established in the literature, its regenerative potential can be exploited against UVA radiation damage.

4. Conclusions and perspectives

The results obtained in this work provided data to study two therapeutic approaches with different mechanisms of action in skin cell culture model under damage induced by ultraviolet radiation A and B.

Both showed no cytotoxic potential in the cells tested, and nanoceria still induced cell proliferation. In addition, both showed antioxidant activity by different mechanisms.

Using assays to evaluate the mechanisms of action, we found that metformin and nanoceria reduced UVA and UVB-induced oxidative damage, which may be related to reduction in cell death by apoptosis.

Thus, it can be concluded that metformin and nanoceria showed promising photoprotective activity by different mechanisms of action, bringing new therapeutic

approaches and serving as a basis for other studies involving its application in the treatment of damage caused by ultraviolet radiation.

ARTIGO CIENTÍFICO 1

Doutoranda: Fabianne Martins Ribeiro

Orientador: Prof. Dr. Celso Vataru Nakamura

Metformin effect on driving cell survival pathway through inhibition of UVB-induced ROS formation in human keratinocytes

Fabianne Martins Ribeiro[a], Bianca Altrão Ratti[b], Fabiana dos Santos Rando[a], Maria Aparecida Fernandez[a], Tânia Ueda-Nakamura[b], Sueli de Oliveira Silva[b], Celso Vataru Nakamura[a,b]*

[a]Programa de Pós-Graduação em Ciências Biológicas, Universidade Estadual de Maringá, Maringá, Paraná, Brazil

[b]Programa de Pós-Graduação em Ciências Farmacêuticas, Universidade Estadual de Maringá, Paraná, Brazil

*Address for correspondence: Celso Vataru Nakamura, Laboratório de Inovação Tecnológica no Desenvolvimento de Fármacos e Cosméticos, Bloco B-08, Universidade Estadual de Maringá, Av. Colombo 5790, CEP 87020-900, Maringá, Paraná, Brazil. Phone number: +55 44 3011-5012, Fax: +55 44 3011-5046. E-mail address: cvnakamura@uem.br

ABSTRACT

Human skin functions go beyond serving only as a mechanical barrier. As a complex organ, the skin is capable to cope with external stressors cutaneous by neuroendocrine systems to control homeostasis. However, constant skin exposure to ultraviolet (UV) radiation causes progressive damage to cellular skin constituents, leading to photoaging, mainly due excessive reactive oxygen species (ROS) production. The present study shows new approaches of metformin (MET), proposing it be repositioned as an antioxidant agent. Currently, MET is the first line treatment of type 2 diabetes and has attracted attention, based on its broad mechanism of action. Therefore, we evaluated MET antioxidant potential in cell-free systems and in UVB irradiated human keratinocyte HaCaT cells. In cell-free system assays MET did not show intrinsic scavenging activity on DPPH• radicals or superoxide ($O_2^{\bullet -}$) xanthine/luminol/xanthine oxidase-generated. Cell-based results demonstrated that MET was able to reduce UVB-induced intracellular ROS and NADPH oxidase-dependent superoxide ($O_2^{\bullet -}$) production. MET posttreatment of HaCaT cells reduced ERK 1/2 phosphorylation, NADPH oxidase activity, and cell death by apoptosis. These findings suggest that the protection mechanism of MET may be through the inhibition of ROS formation enzyme. These results showed that MET might be a promising antioxidant agent against UV radiation induced skin damage.

Keywords: Drug repositioning; ERK 1/2/MAPK; Metformin; MET; Photoaging; UV radiation

1. Introduction

The relevance of aging-related studies of skin goes beyond esthetics. Signs of skin aging, also referred as photoaging, represent a negative impact on quality of life [1]. Longer life expectancy and health conditions associated with aging demand new strategies to access new therapeutic approaches [2]. Thus, as the life span increases, the maintenance of skin health deserves more attention [3].

The human skin tasks are not limited to a barrier to maintain homeostatic functions, but as a complex multifunctional self-regulating organ with neuroendocrine activities such as producing hormones and neurotransmitters that may be essential in response to environmental stress [4]. Along two layers, epidermis and dermis, skin is composed mainly by fibroblasts, keratinocytes and melanocytes, cells that are responsible for the maintenance of skin homeostasis [5]. Cutaneous aging occurs due constant exposure to extrinsic and intrinsic factors leading to cumulative changes and progressive deterioration affecting skin biology [1,6]. The major extrinsic inducer of skin aging is ultraviolet (UV) radiation. UV rays are divided into UVA (320–400 nm) and UVB (280–320 nm) which implies in the effects caused by each type. The most important effect on UVB radiation is DNA damage, acting directly when provoke DNA strand breaks or indirectly when DNA absorbs UVB photons and transfer electrons to other molecules leading to extended ROS production due a chain oxidative reaction [7] which may involve other different sources of ROS, including endoplasmic reticulum, mitochondrial electron transport chain (ETC), and nicotinamide-adenine dinucleotide phosphate (NADPH) oxidases [8], a well-known source of extended UV-induced ROS production [9].

ROS are also known to modulate the mitogen-activated protein kinase (MAPK) signaling pathway. MAPKs, such as extracellular signal–regulated kinase (ERK 1/2) is a critical regulator of the balance between epidermal proliferation, differentiation, and

cell death [10,11]. The consequence of the lack of cell proliferation in these cells hinders the regeneration capacity [12]. Thus, UV radiation can modulate intracellular signaling of ERK 1/2 by induction of ROS, that are mediators of ERK-induced cell death [13].

Metformin (*N*,*N*-dimethylbiguanide) (MET) is a biguanide, derived from the plant *Galega officinalis* (goat's rue), a traditional herbal medicine in Europe [14]. Currently, MET is the most common anti-diabetic drug prescribed to reduce hyperglycemia in type 2 diabetes (T2D) and has aroused increasing interest because of its chemical properties [15]. Moreover, in the context of drug repurposing, several studies have reported its therapeutic potential for novel applications such as anti-cancer, anti-aging, and as regenerative in the wound healing process in young and aged mouse skin [14,16].

However, the approach of repurposing MET as a skin anti-photodamage therapeutic, in *in vitro* HaCaT human keratinocytes cells, under UVB-induced damage have not yet been investigated. In the present study, we evaluated MET potential as a skin antioxidant agent that will provide support to its further clinical applications.

2. Materials and methods

2.1 Chemicals

Dulbecco's modified Eagle's medium (DMEM) and fetal bovine serum (FBS) were obtained from Invitrogen (Grand Island, NY, USA), dimethylsulfoxide (DMSO) were purchased from Synth (Diadema, SP, Brazil). 2',7'-Dichlorodihydrofluorescein diacetate (H_2DCFDA) and Annexin V (FITC conjugate) were purchased from Invitrogen (Eugene, OR, USA). Streptomycin sulfate, penicillin, Hanks' balanced salt solution (HBSS), lucigenin, metformin (MET), camptothecin, NADPH, xanthine,

xanthine oxidase, luminol 2,2-diphenyl-1-picryl-hydrazyl (DPPH), (APO), diphenylene iodonium (DPI), 3-(4,5-dimethylthiazol-2-yl)-2,5-diphenyltetrazolium bromide (MTT), *N*-acetylcysteine (NAC), and rotenone (ROT) were purchased from Sigma Aldrich (St. Louis, MO, USA).

2.2 Cell culture and treatment

HaCaT immortalized keratinocyte cell line was cultured in DMEM supplemented with 10% (v/v) FBS and 1% (v/v) antibiotic solution (100 IU/mL penicillin and 100 µg/mL streptomycin). Cells were incubated at 37 °C in a humidified atmosphere with 5% CO_2 and sub-cultured every 2-3 days to reach exponential growth. For all assays, HaCaT cells were seeded into 6-, 24-, or 96-well microplates at a density of 8×10^5 cells/well, 2.5×10^5 cells/well and 2.5×10^4 cells/well, respectively, and cultured overnight. Different doses of MET (500, 100, 50, 10, 1 µM) or NAC (100 µM) were applied to the cells for 24 h to determine the optimal dosage for further investigations. The 1 h posttreatment was performed with 1 µM MET after UVB irradiation.

2.3 Cell viability assay

Cell viability was measured by MTT assay. Cells were seeded into 96-well plates at a density of 2.5×10^4 cells/well and cultured overnight. Then they were exposed or not to MET (500, 100, 50, 10, and 1 µM) or NAC (100 µM) for 24h. After, 50 µL MTT (2 mg/mL) was added to each well followed by 4 h incubation. The medium was removed and DMSO added to dissolve the formazan crystals. The absorbance was measured at 570 nm in a microplate spectrophotometer (Bio Tek Power Wave XS). Cell viability was calculated relative to the untreated control group.

2.4 UVB irradiation

The cells were irradiated with a UVB lamp (Philips TL 40W/12 RS, The Netherlands) at a distance of 20 cm from the plates. A radiometer equipped with a UVB sensor was used to monitor the radiation dose (detects peak of 312 nm, Vilber Lourmat, VLX-3W).

A dose-response curve (5, 20, 40 and 100 mJ/cm^2, data not shown) was carried out in HaCaT cells and the lowest dose of UVB that significantly caused cell death in 24h without affecting more than 20% of cell viability was chosen. Thus, the dose of 40 mJ/cm^2 was selected for further investigations. For irradiation procedures, the medium was substituted for HBSS buffer.

2.5 Photoprotective assay

Cells were seeded into 6-well microplates at a density of 8× 10^5 cells/well and cultured overnight. After irradiation with UVB (40 mJ/cm^2), cells were treated with MET (100, 10, and 1 µM) or NAC (100 µM) for 1 h and incubated for 24 h in DMEM. Thereafter, the medium was removed, and cell viability was measured by MTT assay. Cell viability was calculated relative to the untreated control group.

2.6 Antioxidant assays

Using a cell-free system, the antioxidant activity was evaluated by hydrogen donor capacity of DPPH$^{\bullet}$ radical [17] and scavenger capacity of superoxide radicals generated by xanthine/luminol/xanthine oxidase (XOD) system as previous described [18]. For both of the methodologies, samples were analyzed at the following concentrations: 1 µM MET, 1 mM APO, 10 µM DPI, 100 µM ROT, and 100 µM NAC.

The scavenging potential on intracellular ROS was measured using C2′,7′-dichlorodihydrofluorescein diacetate (H_2DCFDA). Briefly, HaCaT cells were seeded in

96-well microplates at a density of 2.5×10^4 cells/well and cultured overnight. After irradiation with UVB (40 mJ/cm^2), cells were treated with 1 µM MET for 1 h and 1 mM APO, 10 µM DPI, 100 µM ROT and 100 µM NAC were used as controls. After that, cells were incubated with 5 µM H_2DCFDA for 30 min in the dark at 37 °C. Cell-associated fluorescence was detected after 1 h treatment using a spectrofluorimeter (VICTOR X3, PerkinElmer, USA) equipped with 488/525 nm excitation/emission filters.

2.7 NADPH oxidase assay

Cells were seeded into 6-well microplates at a density of 8×10^5 cells/well and cultured overnight. After irradiation with UVB (40 mJ/cm^2), cells were treated with 1 µM MET for 1 h and 1 mM APO, 10 µM DPI, 100 µM NAC and 10 µM ROT were used as controls. NADPH oxidase activity was measured by lucigenin-dependent chemiluminescence, as a function of $O_2^{\bullet-}$ generated by the NADPH oxidase complex. Briefly, 5×10^5 cells were incubated with 50 µM lucigenin in HBSS buffer. After 5 min the reaction was started by the addition of 200 µM NADPH [19]. Chemiluminescence was measured in white 96-well plates using a luminometer (Spectramax L). The data were expressed in percent of relative light units/5×10^5 cells.

2.8 Western blot analysis

The protein content of HaCaT cells were determined by immunoblotting. Cells were twice washed with phosphate-buffered saline (PBS) and lysed in 150 µL lysis buffer (1 M-Tris-HCl at pH 7.4; 30% glycerin; 5% β-mercaptoethanol; 0.5% SDS v/v) and 1% protease and phosphatase inhibitor cocktail were added. Protein contents in cellular lysates were quantitated according to the Bradford protein assay. The samples were loaded with Laemmli sample buffer (v/v: 62.5 mM Tris-HCl, pH 6.8; 2% SDS;

25% glycerol; 0.01% bromophenol blue; 5% β-mercaptoethanol) and heated for 5 min in a boiling water-bath. Total protein extracts (12 µg) from the cell lysates were separated by 12% SDS–PAGE at 100 V/120 min. A standard molecular weight marker was loaded in parallel. Proteins were transferred from the gel onto a nitrocellulose membrane using the Mini-PROTEAN Tetra Cell (Bio-Rad) and blocked with continuous shaking with 5% BSA in Tween–Tris-buffered saline (20 mM Tris–HCl; 500 mM NaCl; 0.05 % Tween-20 v/v) at room temperature for 60 min. Next, the membrane was incubated overnight at 4 ºC with continuous shaking with 1:100 diluted primary antibodies p-ERK (cat. no. sc-81492), ERK (cat. no. sc-514302), β-actin (sc-69879); all Santa Cruz Biotechnology, Inc., Santa Cruz, California, USA] diluted in 3% BSA in 1X TBST for >12 h at 4 °C. Membrane-bound primary antibodies were detected with 1:10,000 diluted secondary antibodies (sc-2005), Santa Cruz Biotechnology, conjugated to horseradish peroxidase for 1 h at room temperature. The immunoreactive proteins were visualized using an ECL kit (Santa Cruz Biotechnology) and a scanner device (ImageQuant LAS500 GEHealthcare Life Sciences). Image J 1.4 Software (Wayne Rasband, National Institutes of Health) was used to quantify the bands by densitometry, using the β-actin protein expression for normalization.

2.9 Cell apoptosis

Apoptosis was analyzed by flow cytometry using Annexin V-FITC apoptosis detection kit (BD Pharmingen, San Diego, USA), according to the manufacturer's instructions. Cells were seeded into 6-well microplates at a density of 8×10^5 cells/well and cultured overnight. After UVB irradiation (40 mJ/cm^2), cells were treated with 1 µM MET or 10 µM NAC for 1 h and incubated for 24 h in DMEM. Cells were resuspended and washed with binding buffer (140 mM NaCl, 5 mM $CaCl_2$, and 10 mM Hepes–Na, pH 7.4). Afterward, cells were incubated with 5 µL annexin-V FITC in 200

μL binding buffer for 15 min at room temperature, followed by the addition of 4 μL PI (2 μg/mL). Camptothecin (100 μM) was used as a positive control. The analyses were performed in flow cytometry (Attune NxT Flow Cytometer, Life Technologies, Carlsbad, CA, USA). Attune NxT Flow Cytometer software was used for quantitative analysis. A total of 10,000 events were acquired. Cells were considered apoptotic when stained with annexin-V (PI positive or negative).

2.10 Statistical analysis

Experimental data were analyzed by one-way analysis of variance (ANOVA) followed by the Tukey post hoc test. The data were expressed as the mean ± standard deviation (SD) of at least three independent experiments. Values of $p < 0.05$ were considered statistically significant. The statistical analyses were performed using GraphPad Prism 5.0 software (GraphPad, San Diego, CA, USA).

3. Results

3.1 Cytotoxicity and Photoprotective Effect of MET

To evaluate the cytotoxicity effect of MET, HaCaT cells were exposed to different concentrations of MET (500, 100, 50, 10, and 1 μM) for 24 h. The cell viability was determined by the MTT assay. It was observed that cell viability was found to be unaffected by all tested concentrations of MET (Fig. 1A) at 24 h treatment. NAC treatment also did not affect cell viability. Based on the cytotoxicity results assay (Fig. 1A), photoprotective effect of MET on HaCaT cells UVB irradiated were performed with the same concentrations. The results showed that MET at 1 μM protected significantly the cells against viability reduction induced by UVB radiation, increasing 16% of cell viability compared with the UVB group (irradiated and non-

treated cells) (Fig. 1B). Higher MET concentrations (500, 100, 50, or 10 µM) did not significantly enhance protection. Based on these results, 1 µM MET was chosen for further investigations. NAC also protected HaCaT cells (Fig. 2B).

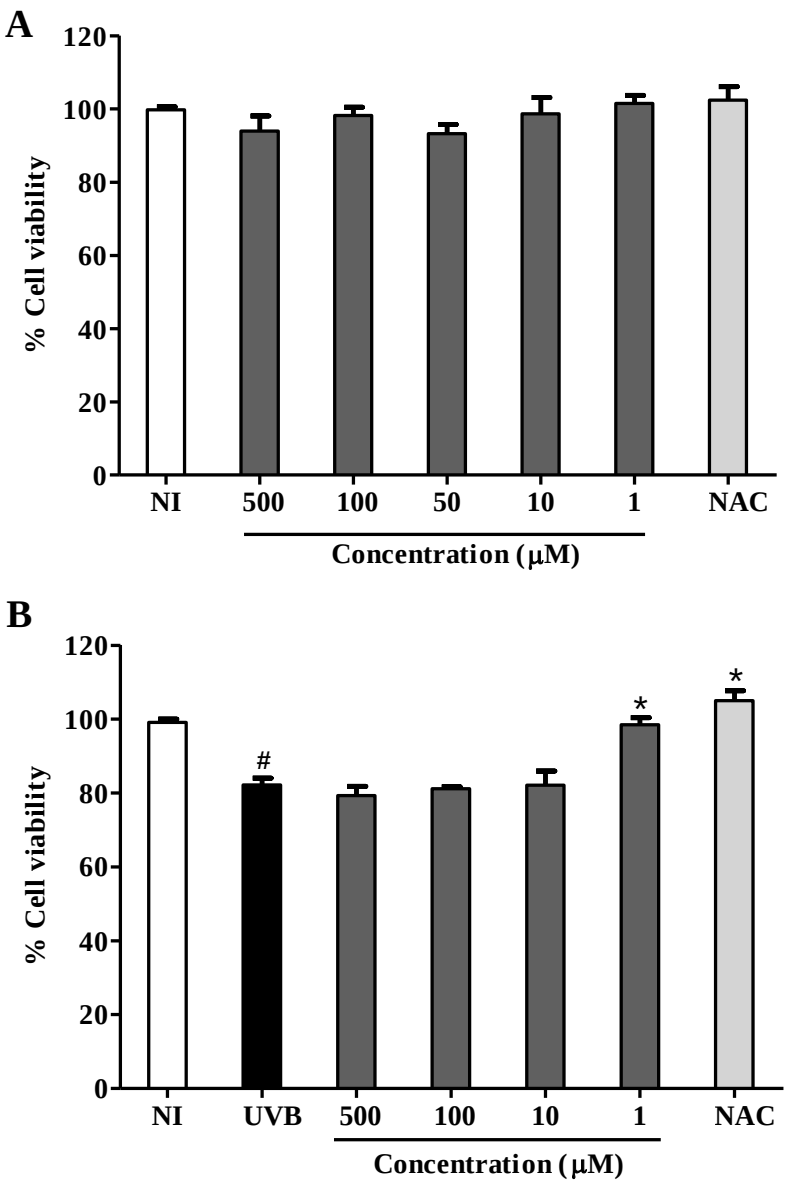

Figure 1. Effects of MET on cell viability. (A) HaCaT cells were treated with 500, 100, 50, 10, and 1 μM MET and 100 μM NAC. After 24h, MTT (2 mg/mL) was added, and readings were performed at 570 nm in a spectrophotometer. (B) Photoprotective effect of MET on HaCaT cells irradiated with UVB (40 mJ/cm^2). Cell viability was evaluated after 24 h of incubation with MET (500, 100, 10, 1 μM) and 100 μM NAC. The results are expressed as a percentage of control nonirradiated cells (NI). Values are means ± SD (n = 3). $^{\#}p \leq 0.05$, significant difference compared with NI group; $^{*}p \leq 0.05$, significant difference compared with UVB group.

3.2 Scavenging Activity of MET in Cell Free Systems

To confirm whether MET may act as both scavenger and NADPH oxidase inhibitor we further evaluated the cell-free antioxidant activity of MET using different

methods based on H-donor capacity and ability to scavenge $O_2^{\bullet-}$ xanthine/XOD-dependent production. We observed that MET was not effective on scavenging DPPH$^{\bullet}$ radicals (5%) (Fig. 2A) and $O_2^{\bullet-}$ (3%) (Fig. 2B), compared with NAC, used as an antioxidant control that inhibited 94% and 72% of DPPH$^{\bullet}$ radicals and $O_2^{\bullet-}$, respectively. APO, DPI and ROT, were able to inhibit approximately 30, 4, and 9%, of H-donor capacity (Fig. 2A), respectively. For $O_2^{\bullet-}$ radicals, APO, DPI, and ROT inhibited approximately 8, 3.5, and 23% (Fig. 2B), respectively. When compared with NAC, the controls did not exhibit antioxidant activity in tested concentrations. Higher concentrations (up to 500 µM) of MET did not show antioxidant activity as well (data not shown).

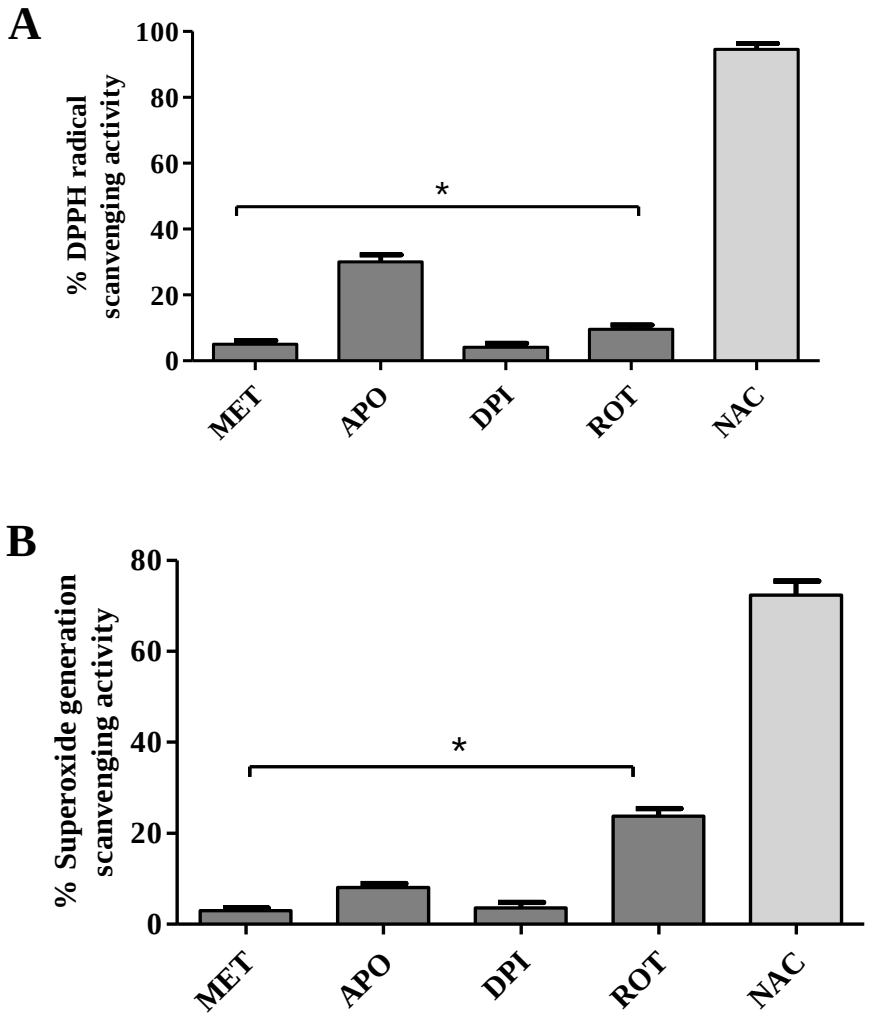

Figure 2. Antioxidant activity of MET. (A) Percent of inhibition of DPPH•. The samples were added to DPPH• (65 μM), followed by incubation for 30 min. Readings were performed in a spectrophotometer at 517 nm. (B) Production of superoxide anion by xanthine/luminol/XOD system. The readings of luminescence were performed in a luminometer plate reader. For both assays the samples were tested at following concentrations: MET 1 μM, APO 1 mM, DPI 10 μM, ROT 10 μM, and NAC 100 μM. The results are expressed as a percentage of control. *$p \leq 0.05$, significant difference compared with NAC group.

3.3 Effect of MET on UVB-induced ROS production in HaCaT cells

To evaluate whether the cytoprotective effect observed for MET is due its ROS scavenger activity, we measured the UVB-induced ROS production in HaCaT cells treated with MET using the H_2DCFDA fluorescence assay. Figure 3A shows substantial increase on ROS production (72%) in the UVB group compared with nonirradiated cells

(NI), and MET treatment significantly reduced this increase to just 39%. APO, DPI, ROT, and NAC decreased 55, 54, 31, and 68% of UVB-induced ROS production, respectively (Fig. 3A). For all treated and nonirradiated cells, ROS production was not observed compared with nonirradiated cells (NI).

We also tested NADPH oxidase-dependent superoxide ($O_2^{\bullet-}$) production in HaCaT cells UVB-irradiated. UVB radiation increased 69% of $O_2^{\bullet-}$ production while posttreatment with MET decreased 44% of $O_2^{\bullet-}$ production compared with UVB group (Fig 3B). APO, DPI, ROT and NAC decreased 60%, 58%, 3% and 70% of UVB-induced $O_2^{\bullet-}$ production, respectively (Fig. 3B). MET did not alter the level of $O_2^{\bullet-}$ in nonirradiated cells.

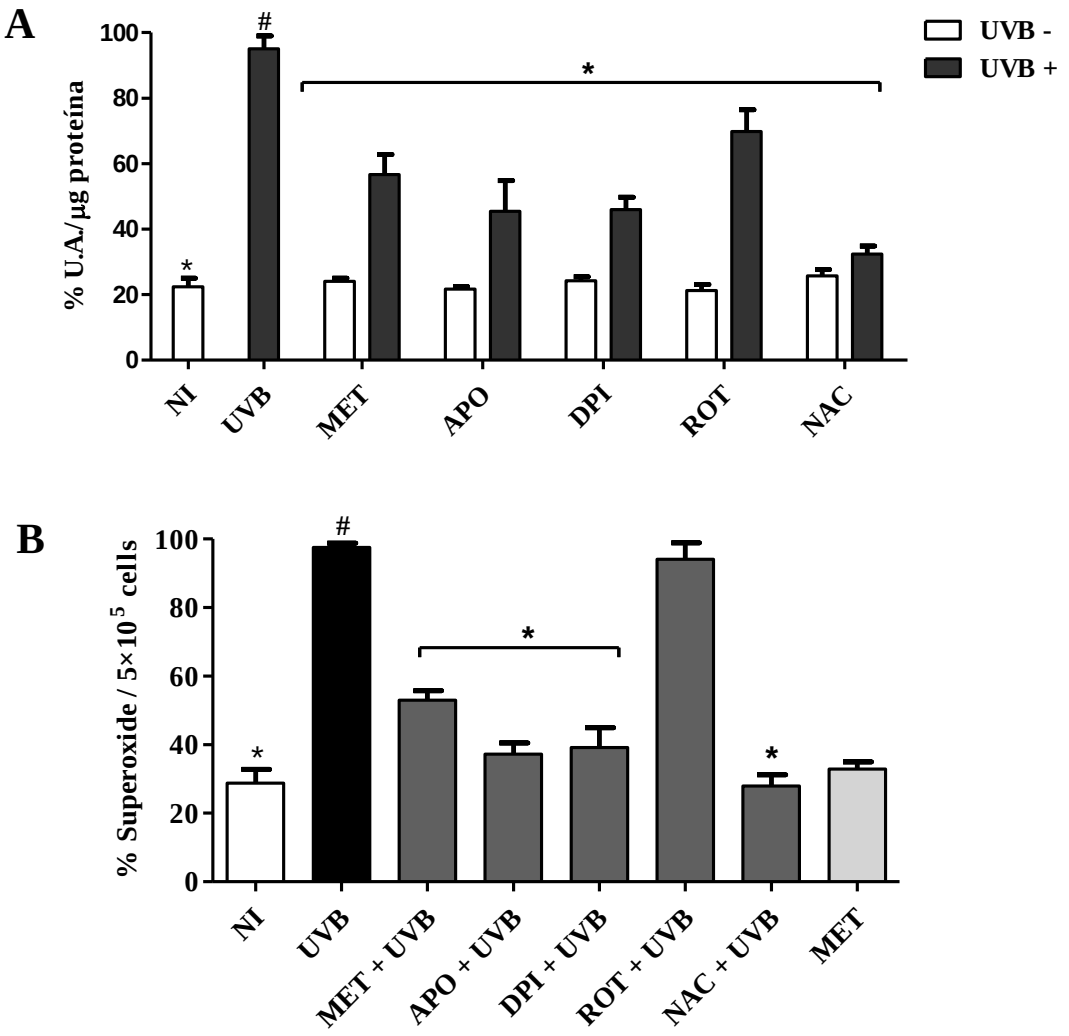

Figure 3. Effect of MET on oxidizing species production in HaCaT cells. (A) Intracellular ROS production. Cells were irradiated (40 mJ/cm^2) and treated with MET 1 µM, APO 1 mM, DPI 10 µM, NAC 100 µM, and ROT 10 µM for 1 h followed by readings. (B) Effect of MET on generation of superoxide anions by NADPH oxidase. Cells were irradiated (40 mJ/cm^2) and treated with MET 1 µM, APO 1 mM DPI 10 µM, and NAC 100 µM for 1 h. NI, untreated and nonirradiated cells; UVB, untreated and irradiated cells with UVB. Superoxide anion production was measured by the lucigenin-enhanced chemiluminescence. $^{\#}p \leq 0.05$, significant difference compared with untreated and nonirradiated cells (NI); $^{*}p \leq 0.05$, significant difference compared with UVB group.

3.4 UVB-induced increase of phosphorylated ERK 1/2 is reduced by MET treatment

To show whether MET protective cell death effect involve MAPK pathway we evaluated ERK 1/2 using Western blot. UVB significantly induced ERK 1/2 phosphorylation (Fig. 4). Both, MET and NAC significantly reduced the UVB-induced

phosphorylation of ERK 1/2 by 25% and 40%, respectively (Fig. 4). Figure 5 shows that ERK 1/2 expression remained sustained even 24 h after UVB irradiation.

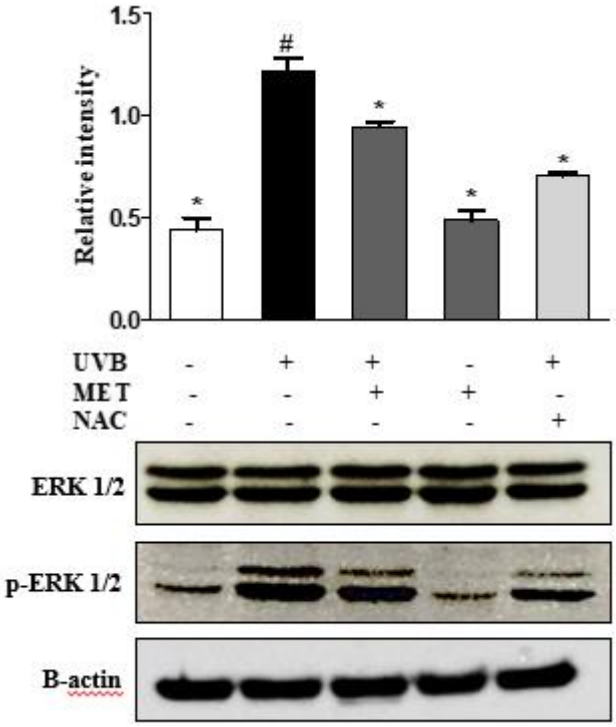

Figure 4. ERK 1/2 phosphorylation expression in HaCaT cells following MET treatment. Cells were irradiated (40 mJ/cm^2) and treated or not with 1 μM MET and 100 μM NAC for 1 h followed by 24 h incubation. Total protein was isolated and probed with antibodies for ERK 1/2, p-ERK 1/2 and β-Actin. Graphs indicate the relative band intensities, as determined by ImageJ software and plotted as the means ±SD. of three independent experiments. *$p \leq 0.05$, significant difference compared with UVB group.

3.5 MET protected HaCaT cells against UVB-induced apoptosis

As known NADPH oxidase are involved in the process of UV-extended ROS production [20]. The inhibition of NADPH oxidase might be a way to deal with the UVB induced cell death such as apoptosis. Thus, we evaluated the effect of MET on apoptosis cell death using Annexin V/PI. The percentage of apoptotic cells were significantly increased by UVB radiation (15%) compared with nonirradiated cells (NI) (Fig 5A, B). Posttreatment of HaCaT with MET showed a statistically significant

protection against UVB-induced apoptosis cell death, decreasing apoptosis to a similar level as the NI group (Fig 5A, B). Cell survival of MET treatment in nonirradiated cells (MET group) remained unaffected compared with the NI group. NAC treatment was also evident on UVB-induced apoptosis. Camptothecin (CAMP), used as positive control, also induced significant increased apoptosis.

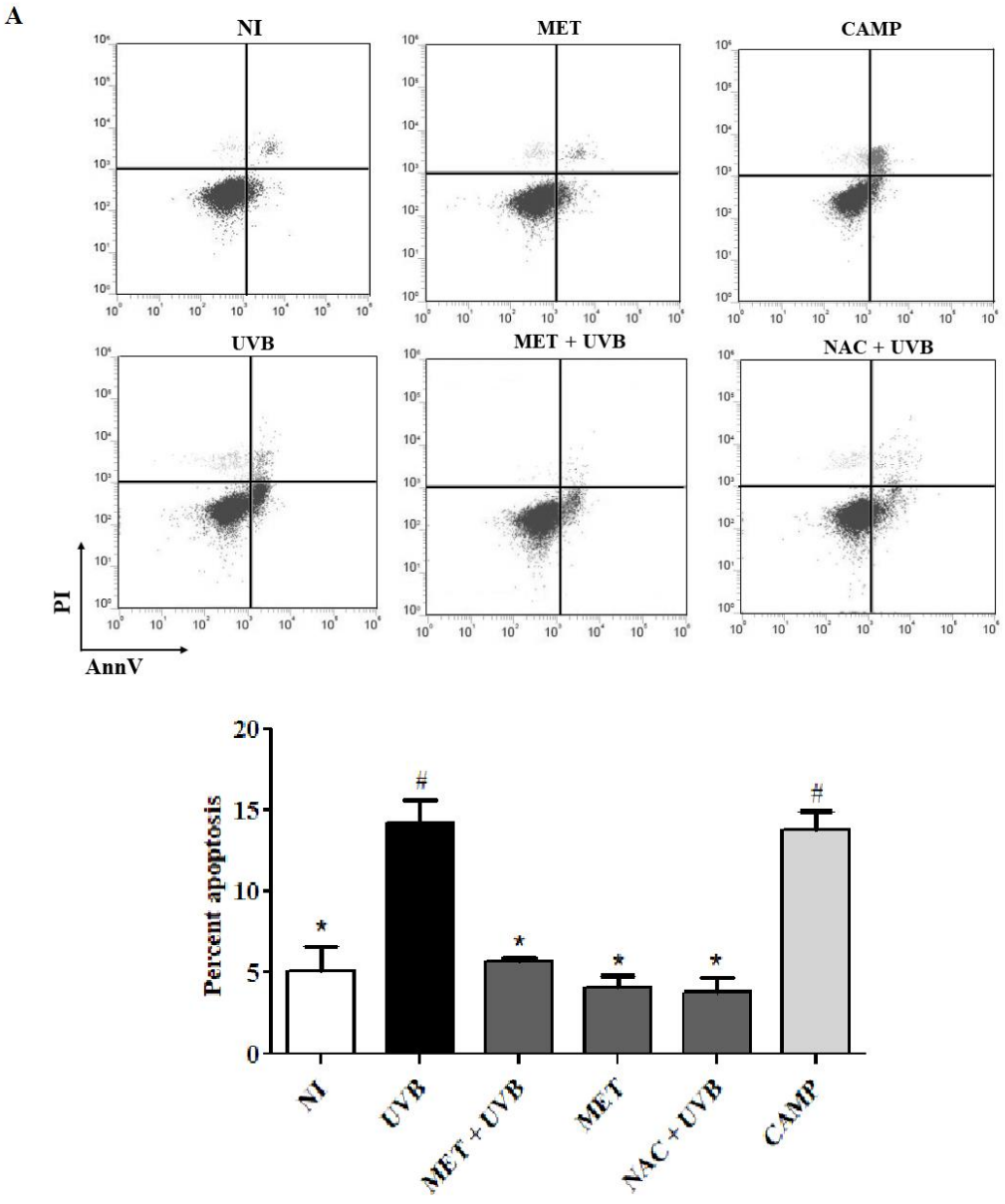

Figure 5. Evaluation of cell death by apoptosis using annexin V-FITC/PI staining. (A, B) Cells were irradiated (40 mJ/cm^2) and treated or not with MET 1 µM and NAC 100 µM for 1 h followed by 24 h incubation and flow cytometric analysis. NI: untreated and nonirradiated cells; UVB: untreated and irradiated cells with UVB. Values are means ± SD (n = 3). Typical histograms of at least three independent experiments are depicted. $^{\#}p \leq 0.05$, significant difference compared with NI group; $^{*}p \leq 0.05$, significant difference compared with UVB group.

4. Discussion

The present study aimed to investigate the protection mechanism of MET against UVB induced damage in human keratinocytes cells. We have demonstrated that

MET may indirectly reduce intracellular ROS production through inhibition of NADPH oxidase and by decreasing on ERK 1/2 phosphorylation, one critical regulator of cell proliferation and cell death [21].

Although mechanisms of action of MET are not fully understood, it is widely prescribed in type 2 diabetes treatment as the first line antidiabetic agent [22]. Several studies have shown a therapeutic approach of MET that has attracted the attention of studies of age-related diseases, modulating the biology of aging and promoting health and longevity based on the rejuvenating effect [23]. UV radiation is known to induce damage in the skin, mainly by induction of ROS that may lead to oxidative stress and cell death [24].

To reveal the mechanism by which MET protects cells under UVB irradiation, we first focused on its antioxidant activity. Here, we have demonstrated that MET did not show intrinsic antioxidant activity in cell-free systems evidenced by the DPPH and xanthine assay. However, MET reduced levels of UVB induced intracellular ROS and NADPH oxidase-dependent superoxide ($O_2^{\bullet-}$) in live cells similar to Apo and DPI, well-known NADPH oxidase inhibitors. NADPH oxidase system is an enzymatic system that produces superoxide anion through the consumption of molecular oxygen [25]. Thus, the inhibitory effect of MET on UVB induced ROS formation might be due a direct MET inhibitory effect on NADPH oxidase activation. Recent studies have shown that MET enhances antioxidant enzymes such as SOD, CAT and GSH *in vitro* and *in vivo*, therefore its antioxidant activity might be closely related to upregulating antioxidant gene expression [26]. This is also consistent with a previous suggestion of the role of MET on decreasing ROS production through reduction of NADPH oxidase activity in renal cells under oxidative stress *in vitro* and *in vivo* [27].

Interestingly, our data shows that ROT, an inhibitor of mitochondrial complex I (NADH: ubiquinone oxidoreductase), led to a decrease in intracellular ROS. This

intrinsic scavenge activity was not observed in the cell-free systems (DPPH and XOD system). These data might evidence the UVB-induce mitochondrial ROS formation. Several MET-related studies have focused on mitochondria [22]. As a relatively hydrophilic and positively charged molecule, MET crosses the plasma membrane and accumulates by membrane-driven-potential in the mitochondrial matrix [28]. Thus, MET might be protecting cells from UVB induced ROS production by both, decreasing NADPH oxidase activity and inhibiting the ROS mitochondrial.

We also showed that MET significantly decreased the levels of p-ERK protein and decrease the apoptosis on UVB induced HaCaT even after 24 h of irradiation. These data might be once again related to the antioxidant effect of MET. The treatment with the antioxidant NAC also significantly decreased ERK phosphorylation, suggesting even more the involvement of ROS in ERK activation [29]. It is known that UV radiation activates signal transduction cascades, such as ERK 1/2 MAPK, which regulates the induction or repression of cell survival and apoptosis, either directly or via ROS generation [30][31]. ERK 1/2 regulates cell growth and differentiation and its phosphorylation depends on the activation signal intensity [32]. The over p-ERK 1/2 activation blocks cell cycle entry and inhibits cell proliferation that is required for promoting apoptosis [33,34]. These data is supported by an earlier study that showed the decrease on ERK activation by metformin in the mice skin model that had been chronically exposed to UVB radiation [35].

Some studies showed that MET can induce the increase of ROS formation and apoptosis [36]. This dual effect is highly dependent on the concentration of MET used. Many studies were based on experimental supra-pharmacological doses of metformin reaching up to 100 times more than the therapeutic (80μM) dose used in type 2 diabetes treatment [21].

Previous studies support our belief on metformin anti-photoageing therapeutic potential of metformin as shown by Lee et al (2010) [37] that metformin pretreatment reduced MMP-9 expression in skin by negative regulation of Sirt1 induced by a dose of 30 mJ/cm^2 of UVB.

5. Conclusion

Our results suggest that the protection mechanism of MET on UVB-irradiated HaCaT cells is due to the reduction of ROS through the direct inhibition of ROS formation enzymes such as NADPH oxidase and consequent inactivation of sustained ERK 1/2 MAPK to protect cells from apoptosis (Fig 6). MET, as an antioxidant agent, provides a new approach and new insights into UVB-induced skin disorders and potential targets for therapeutic interventions by targeting potential sources of ROS.

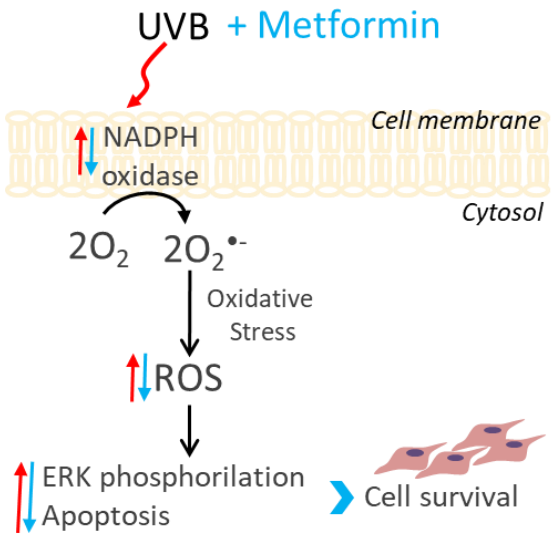

Figure 6: Photoprotective mechanism of metformin (blue arrows) against UVB-induced ROS formation in HaCaT cells (red arrows).

Acknowledgements

This study was supported by grants from the Coordenação de Aperfeiçoamento de Pessoal de Nível Superior - Brasil (CAPES) – (Finance Code 001); COMCAP-UEM

(Complex of Research Support Centers), Conselho Nacional de Desenvolvimento Científico e Tecnológico, PRONEX/Fundação Araucária and Financiadora de Estudos e Projetos.

References

[1] M.A. Farage, K.W. Miller, P. Elsner, H.I. Maibach, Characteristics of the Aging Skin, Adv. Wound Care. 2 (2013) 5–10. doi:10.1089/wound.2011.0356.

[2] W.M. Valencia, A. Palacio, L. Tamariz, H. Florez, Metformin and ageing: improving ageing outcomes beyond glycaemic control, Diabetologia. 60 (2017) 1630–1638. doi:10.1007/s00125-017-4349-5.

[3] K. Christensen, G. Doblhammer, R. Rau, J.W. Vaupel, Ageing populations: the challenges ahead, Lancet. 374 (2009) 1196–1208. doi:10.1016/S0140-6736(09)61460-4.

[4] G. Bocheva, R.M. Slominski, A.T. Slominski, Neuroendocrine Aspects of Skin Aging, Int. J. o f Mol. Sci. (2019) 1–19. doi:10.3390/ijms20112798.

[5] A. Pagani, M.M. Aitzetmüller, E.A. Brett, V. König, R. Wenny, D. Thor, C. Radtke, G.M. Huemer, H.-G. Machens, D. Duscher, Skin Rejuvenation through HIF-1α Modulation, Plast. Reconstr. Surg. 141 (2018) 600e-607e. doi:10.1097/PRS.0000000000004256.

[6] T. Quan, G.J. Fisher, Role of age-associated alterations of the dermal extracellular matrix microenvironment in human skin aging: A mini-review, Gerontology. 61 (2015) 427–434. doi:10.1159/000371708.

[7] Tüzün Y, Kutlubay Z,Engin B, Serdaroğlu S. Basal Cell Carcinoma. In: Xi Y, editor. Skin Cancer Overview. Croatia: InTech; 2011. Available from: http://www.intechopen.com/books/skin-cancer-overview/basal-cell-carcinoma .

[8] S. Zhang, E. Duan, Fighting against Skin Aging, Cell Transplant. (2018) 096368971772575. doi:10.1177/0963689717725755.

[9] A. Fedoriw, J. Mugford, Development and Homeostasis of the Skin Epidermis Development and Homeostasis of the Skin Epidermis, Spring. (2012) 1–19. doi:10.1101/cshperspect.a008383.

[10] Y. Jang, S.H. Jeong, Y.H. Park, H.C. Bae, H. Lee, W.I. Ryu, G.H. Park, S.W. Son, UVB induces HIF-1α-dependent TSLP expression via the JNK and ERK pathways, J. Invest. Dermatol. 133 (2013) 2601–2608. doi:10.1038/jid.2013.203.

[11] M.C. Velarde, M. Demaria, Targeting senescent cells: Possible implications for delaying skin aging: A mini-review, Gerontology. 62 (2016) 513–518. doi:10.1159/000444877.

[12] S. Cagnol, J. Chambard, MINIREVIEW ERK and cell death : Mechanisms of ERK-induced cell death – apoptosis , autophagy and senescence, 2 (2010) 2–21. doi:10.1111/j.1742-4658.2009.07366.x.

[13] R. Pryor, F. Cabreiro, Repurposing metformin : an old drug with new tricks in its binding pockets, (2015) 307–322. doi:10.1042/BJ20150497.

[14] B. Viollet, B. Guigas, N.S. Garcia, J. Leclerc, M. Foretz, F. Andreelli, Cellular and molecular mechanisms of metformin : an overview, 270 (2012) 253–270. doi:10.1042/CS20110386.

[15] S.J. Griffin, J.K. Leaver, G.J. Irving, S.J. Griffin, Impact of metformin on cardiovascular disease : a meta-analysis of randomised trials among people with type 2 diabetes, (2017) 1620–1629. doi:10.1007/s00125-017-4337-9.

[16] P. Zhao, B. Sui, N. Liu, Y. Lv, C. Zheng, Y. Lu, W. Huang, C. Zhou, J. Chen, D. Pang, D. Fei, K. Xuan, C. Hu, Anti-aging pharmacology in cutaneous wound

healing: effects of metformin, resveratrol, and rapamycin by local application, (2017) 1–11. doi:10.1111/acel.12635.

[17] W. Brand-Williams, M.E. Cuvelier, C. Berset, Use of a free radical method to evaluate antioxidant activity, LWT - Food Sci. Technol. 28 (1995) 25–30. doi:10.1016/S0023-6438(95)80008-5.

[18] F.M. Ribeiro, H. Volpato, D. Lazarin-Bidóia, V.C. Desoti, R.O. de Souza, M.J.V. Fonseca, T. Ueda-Nakamura, C.V. Nakamura, S. de O. Silva, The extended production of UV-induced reactive oxygen species in L929 fibroblasts is attenuated by posttreatment with Arrabidaea chica through scavenging mechanisms, J. Photochem. Photobiol. B Biol. 178 (2018) 175–181. doi:10.1016/j.jphotobiol.2017.11.002.

[19] Y.S. Kim, M.J. Morgan, S. Choksi, Z. gang Liu, TNF-Induced Activation of the Nox1 NADPH Oxidase and Its Role in the Induction of Necrotic Cell Death, Mol. Cell. 26 (2007) 675–687. doi:10.1016/j.molcel.2007.04.021.

[20] A. Valencia, I.E. Kochevar, Nox1-Based NADPH Oxidase Is the Major Source of UVA-Induced Reactive Oxygen Species in Human Keratinocytes, 128 (2008). doi:10.1038/sj.jid.5700960.

[21] L. He, F.E. Wondisford, Metformin action: Concentrations matter, Cell Metab. 21 (2015) 159–162. doi:10.1016/j.cmet.2015.01.003.

[22] G. Rena, D.G. Hardie, E.R. Pearson, The mechanisms of action of metformin, (2017) 1577–1585. doi:10.1007/s00125-017-4342-z.

[23] M.G. Novelle, A. Ali, C. Diéguez, M. Bernier, R. de Cabo, Metformin: A hopeful promise in aging research, Cold Spring Harb. Perspect. Med. 6 (2016) 1–12. doi:10.1101/cshperspect.a025932.

[24] U. Light, I. Generation, R.O. Species, Ultraviolet Light Induced Generation of Reactive Oxygen Species, (n.d.) 15–23.

[25] F. Jiang, Y. Zhang, G.J. Dusting, NADPH Oxidase-Mediated Redox Signaling: Roles in Cellular Stress Response, Stress Tolerance, and Tissue Repair, Pharmacol. Rev. 63 (2011) 218–242. doi:10.1124/pr.110.002980.

[26] S.W. Choi, C.K. Ho, Antioxidant properties of drugs used in Type 2 diabetes management: could they contribute to, confound or conceal effects of antioxidant therapy?, Redox Rep. 23 (2018) 1–24. doi:10.1080/13510002.2017.1324381.

[27] X. Yang, H. Ding, Z. Qin, C. Zhang, S. Qi, H. Zhang, T. Yang, Z. He, K. Yang, E. Du, C. Liu, Y. Xu, Z. Zhang, Metformin Prevents Renal Stone Formation through an Antioxidant Mechanism in Vitro and in Vivo, Oxid. Med. Cell. Longev. 2016 (2016). doi:10.1155/2016/4156075.

[28] E. Fontaine, Metformin-Induced Mitochondrial Complex I Inhibition: Facts, Uncertainties, and Consequences, Front. Endocrinol. (Lausanne). 9 (2018) 23–28. doi:10.3389/fendo.2018.00753.

[29] Y. Son, Y.-K. Cheong, N.-H. Kim, H.-T. Chung, D.G. Kang, H.-O. Pae, Mitogen-Activated Protein Kinases and Reactive Oxygen Species: How Can ROS Activate MAPK Pathways?, J. Signal Transduct. 2011 (2011) 1–6. doi:10.1155/2011/792639.

[30] J. Ortonne, R. Ballotti, W. Englaro, B. De, Solar ultraviolet light activates extracellular signal-regulated kinases and the ternary complex factor in human normal keratinocytes, (1998) 661–664.

[31] A.M.B. and Z. Dong, Mitogen-Activated Protein Kinase Activation in UV-Induced Signal Transduction, Sci. STKE. (2003) 91–98.

doi:10.1126/stke.2003.167.re2.

[32] Y. Mebratu, Y. Tesfaigzi, How ERK1/2 activation controls cell proliferation and cell death is subcellular localization the answer?, Cell Cycle. 8 (2009) 1168–1175. doi:10.4161/cc.8.8.8147.

[33] Y.-J. Lee, H.-N. Cho, J.-W. Soh, G.J. Jhon, C.-K. Cho, H.-Y. Chung, S. Bae, S.-J. Lee, Y.-S. Lee, Oxidative stress-induced apoptosis is mediated by ERK1/2 phosphorylation, Exp. Cell Res. 291 (2003) 251–266. doi:10.1016/S0014-4827(03)00391-4.

[34] C. López-camarillo, E.A. Ocampo, M.L. Casamichana, Protein Kinases and Transcription Factors Activation in Response to UV-Radiation of Skin : Implications for Carcinogenesis, (2012) 142–172. doi:10.3390/ijms13010142.

[35] C.L. Wu, L. Qiang, W. Han, M. Ming, B. Viollet, Y.Y. He, Role of AMPK in UVB-induced DNA damage repair and growth control, (2013) 2682–2689. doi:10.1038/onc.2012.279.

[36] R.--erk Inactivation, X. Wang, R. Li, X. Zhao, X. Yu, Q. Sun, Metformin Promotes HaCaT Cell Apoptosis through Generation of Reactive Oxygen Species, (2018). doi:10.1007/s10753-018-0749-z.

[37] J. Lee, K. Park, H. Min, S.J. Lee, J. Kim, J. Choi, W. Kim, H. Cha, Negative regulation of stress-induced matrix metalloproteinase-9 by Sirt1 in skin tissue, 1 (2010) 1060–1066. doi:10.1111/j.1600-0625.2010.01129.x.

ARTIGO CIENTÍFICO 2

Doutoranda: Fabianne Martins Ribeiro

Orientador: Prof. Dr. Celso Vataru Nakamura

Effect of cerium oxide nanoparticles on fibroblasts L929 proliferation, aging and death: Further studies on protective mechanisms against UVA-induced damage

Fabianne Martins Ribeiro[a], Mariana Maciel de Oliveira[b], Sudipta Seal, Tânia Ueda-Nakamura[b], Sueli de Oliveira Silva[b], Celso Vataru Nakamura[a,b]*

[a]Programa de Pós-Graduação em Ciências Biológicas, Universidade Estadual de Maringá, Maringá, Paraná, Brazil

[b]Programa de Pós-Graduação em Ciências Farmacêuticas, Universidade Estadual de Maringá, Paraná, Brazil

[c]Advanced Materials Processing and Analysis Centre, Nanoscience Technology Center, University of Central Florida, Orlando, FL, US

*Address for correspondence: Celso Vataru Nakamura, Laboratório de Inovação Tecnológica no Desenvolvimento de Fármacos e Cosméticos, Bloco B-08, Universidade Estadual de Maringá, Av. Colombo 5790, CEP 87020-900, Maringá, Paraná, Brazil. Phone number: +55 44 3011-5012, Fax: +55 44 3011-5046. E-mail address: cvnakamura@uem.br

ABSTRACT

Exposure to ultraviolet radiation is responsible for premature skin aging and carcinogenesis mainly driven by overproduction of ROS. There is growing interest for research on new strategies that address the photoaging prevention such as the approach of using nanomaterials. Cerium oxide nanoparticles (nanoceria) show enzyme-like activity on scavenging ROS. Fibroblasts cells L929 were treated with nanoceria (100 nM) and exposed to UVA radiation and assayed for cell viability, oxidative stress by evaluation of ROS production, SOD and GSH activity and cell death and proliferation. Pretreatment of cells with nanoceria showed no cytotoxicity and protected cells from UVA-induced death by increasing of cell viability. Nanoceria also decreased ROS production imediately after irradiation or for up to 48 h and restored SOD and GSH activity. Additionally, nanoceria treatment prevented apoptosis by decreasing Caspase 3/7 levels and mitochondrial membrane potential loss. Nanoceria significantly improved cell survival by increasing of proliferation for 5 days compared with non-irradiated and in UVA-irradiated cells and in wound healing assay. Furthermore, it was found that nanoceria decreased cell aging and ERK 1/2 phosphorylation. Our study suggests that nanoceria might be a potential ally with the intracellular antioxidant enzymes to fight UVA-induced photodamage and consequently drive cells to survival and proliferate mechanisms.

Keywords: cerium oxide nanoparticles, nanoceria, ultraviolet radiation, antioxidant, wound healing

1. Introduction

Nanotechnology have attracted attention in diferent fields of Science including medicine and pharmacology. Special attention has been paid to the development of nanoparticles (NPs) enzyme-like activities, refered as nanozymes [1]. Mimicking natural enzymes, nanozymes offers several advantages such as low cost, high stability, better catalytic efficiency [1,2].

Cerium oxide oxide nanoparticles (CNPs or nanoceria) are particularly interesting in a wide range of biomedical applications due its antioxidant properties. Several studies support CNPs cytoprotective efficacy suggesting that CNPs reduce chronic inflammation, promote angiogenesis, promote tissue regeneration, decrease cell death and increase life span [3,4]. Cerium (Ce) is the unique metal that can exist in both valence state (Ce^{3+}/Ce^{4+}). This allows CNPs to have self-regenerative redox cycling property possibiliting store and release oxygen (O_2) in his surface, combining CAT- and SOD-mimetic activities, remaining active for an extended time and thereby protecting cells against the harmuful effect of excessive reactive oxyegen species (ROS) production [5,6].

The ultraviolet radiation (UV) is a well-known ROS inducer in human skin contributing to the development of several chronic diseases and aging process [7]. The effects of ultraviolet A rays (UVA, 320–400 nm) are well recognized as the mainly responsable for driven skin cells to senescence through the ROS-induced damage of essencial cell macromolecules, including lipids, proteins and nucleic acids affecting antioxidant cellular defense systems and dysregulating important cell-signaling pathways [11] in skin deep layers affecting mainly fibroblasts [8]. These cells are the major cell type in the dermis and play a pivotal role in skin physiology [15]contribute to extracellular-matrix (ECM) and collagen production to maintain the structural integrity of skin playing an important role in cutaneous wound healing process [9]. In recent

years, various studies have been conducted on the role of fibroblasts on wound healing and how this process can be disrupted by UVA radiation [10–12].

Although a recent study showed that CNPs protect fibroblasts from UVA-induced oxidative damage through antioxidant properties we believe that besides that CNPs could also modulate signaling patways of cellular proliferation. Thus, our goal was to study the ability of CNPs induce fibroblasts proliferation under UVA radiation. Our data showed that CNPs decrease UVA-induced fibroblast death through the redox cell balance restoration setting off signal-regulated protein kinases 1 and 2 (ERK1/2) that control both, cell proliferation and apoptotic pathways contributing to cell proliferation.

2. Material and Methods

2.1 CNP synthesis and characterization

Cerium oxide nanoparticles (CNP) were synthesized using the earlier established protocol using wet chemistry approach in the size range of 3-5 nm and concentration 5 mM, as described in our earlier publication [13]. In brief, quantified amount of cerium nitrate hexahydrate salt was dissolved in ultrapure DI water and stoichiometric amount of hydrogen peroxide solution (H_2O_2) was added to the solution. This induces the oxidation of cerium ions into formation of ultra-small CNP in the size range of 3-5 nm.

Physiochemical characterization of these CNP were performed using High resolution transmission electron microscopy (HRTEM; Philips Tecnai), Hydrodynamic radius and the surface charge (zeta potential) using a zeta sizer (Nano-ZS from Malvern Instruments).

2.2 Uptake assay

To determine the best time of CNP treatment and assess the cellular uptake, L929 cells were treated with FITC-CNP for 1, 2 and 24 h. Cells were detached via trypsinization and analyzed by flow cytometry (FACSCalibur).

2.3 Cell culture, treatment and UVA irradiation

The experiments were conducted using the mouse fibroblast cell line L929 (ATCC® CCL1™, Manassas, USA) cultured in DMEM (Dulbecco's modified Eagle's medium, Life Technologies/Gibco Laboratories, Grand Island, NY, USA) containing 10.0% fetal bovine serum (FBS, Life Technologies/Gibco Laboratories, Grand Island, NY, USA), 2 mM L-glutamine at 37°C in a 5% CO_2 atmosphere. For all experiments, L929 cells were seeded at a density of 2.5x105 cells/mL and were below 20 passages.

For cytotoxicity, photoprotection and mitochondrial membrane potential ($\Delta\psi m$) measurement assays, cells were seeded into 96-well plates. For wound healing, cell growth, β-galactosidase (SA-βG) and cell death assays, cells were seeded into 24-well plate. For other experiments, cells were seeded into 6-well plates. Cell monolayres were washed 3 times with Phosphate-Buffered Saline buffer (PBS), treated with CNP 100 nM diluted in serum-free DMEM for 24 h at 37 °C in a humidified atmosphere with 5% CO_2 followed by irradiation.

For irradiation procedure, cells were washed with PBS and irradiated with Hank's balanced salt solution (HBSS, Sigma-Aldrich, St. Louis, MO, USA) at intermittent dose of 15 J/cm^2 or with a unique dose of 30 J/cm^2 of UVA lamps (Philips

TLK 40W/10R lamp, The Netherlands) monitored using a radiometer sensor (peak: 365 nm, VLX-3W, Vilber Lourmat, Marne La Vallée, France). After irradiation, HBSS was changed by DMEM serum-free and cells were immediately assayed or maintained in an incubator at 37 °C in a humidified atmosphere with 5% CO_2 for the time required for each assay. N-Acetylcysteine (NAC, 100 µM-1 h treatment, Sigma-Aldrich, St. Louis, MO, USA) was used as antioxidant control.

2.4 Citotoxicity and Photoprotection assay

To assess the cytotoxic potential of the CNP we employed the MTT assay. Briefly, L929 cells were treated with samples in various concentrations of 500, 100, 50, 10 and 5 nM for 24 h at 37˚C in a humidified 5% CO_2 incubator. After, cells were washed with PBS and 50 µL of MTT (2 mg/mL) was added for 4 h. The measured was performed at the absorbance of 570 nm (BioTek, PowerWave XS microplate spectrophotometer) and the percentage of cell viability was determined relative to the untreated control group.

To assess UVA phototoxicity, L929 cells were treated with 100, 50, 10 and 5 nM CNP for 24h. After, the CNP solution was replaced with HBSS and cells were irradiated with UVA (30J/cm^2) and then incubated with serum-free DMEM for 24 h. After, cytotoxicity was detected by MTT assay.

2.5 Measurement of intracelular ROS

Intracellular ROS was measured using C2′,7′-dichlorodihydrofluorescein diacetate (H_2DCF-DA, Eugene, OR, USA). Briefly, L929 cells were treated with 100 nM CNP for 24 h or 100 µM N-acetylcysteine (NAC), 100 UI superoxide dismutase (SOD, Sigma-Aldrich, St. Louis, MO, USA) and 100 UI catalase (CAT, Sigma-Aldrich, St. Louis, MO, USA) for 1 h and irradiated with UVA at a unique dose of 30 J/cm^2 or

with 15 J/cm^2 followed by an additional dose (15 J/cm^2) after 24 h. After different time, cells were incubated with 5 μM H_2DCF-DA for 30 min in the dark at 37 °C. Cell-associated fluorescence was detected using a spectrofluorimeter (VICTOR X3, PerkinElmer, USA, λex = 488 nm, λem = 525 nm). The fluorescence precentage was expressed as arbitrary fluorescence units per μg of protein dertermined by Bradford method (Bio-Rad, CA, USA).

2.6 Intracelular antioxidant enzymes activity measurements

To evaluate intracelular antioxidant enzymes activity, after 100 nM CNP or 100 μM NAC treatment, L929 cells were irradiated with UVA (30 J/cm^2) and incubated for 1 h. Cells were resuspended and lysated in cold Tris buffer (Tris 10 mM, pH=7,4), sonicated for 60 seconds with a 30% pulse. The cell debri was removed by centrifugation at 14,000 rpm for 10 minutes at 4 ºC and the supernatants were assayed for GSH levels and SOD activity. Protein concentration was determined by Bradford method.

To measure GSH levels *o*-phthalaldehyde (OPT, Sigma-Aldrich, St. Louis, MO, USA) was used. Cell lysate supernant (50 μg/mL of protein) was transferred to a black 96-well microplate containing sodium phosphate buffer (100 mM KH_2PO_4–KOH, pH 10, 185 μl) followed by 10 μl OPT (10 mg/ml in ice cold methanol) addition. After 25 min of incubation in the dark with gentle mixing, the plate was readed in a fluorescence plate reader (VICTOR X3, PerkinElmer, USA, λex = 350 nm, λem = 420 nm) [14].

The enzimatic SOD activity was determined by measuring the inhibition of pyrogallol autoxidation. In brief, 930 μL of Tris buffer (200 mM Tris, 2 mM EDTA, pH 8.2) and 50 μg of protein of cell lysate were mixed followed by addition of 70 μl pyrogallol solution (15 mM in 1 mM Tris-HCL, pH 8.2) and the absorbance was readed

at 420 nm (Shimadzu, UV-1700). One unit of SOD activity was considered based on 50% of the pyrogallol oxidation (expressed as unit of SOD/μg protein).

2.7 Cell Growth Assay

The L929 cells were treated with 100 nM of CNP for 24h or 10μM of NAC for 1 h, irradiated with UVA (30 J/cm^2) and the cells were collected by trypsinization right after irradiation or after incubation for 1, 2, 3, 4 and 5 days and counted in a Neubauer chamber using the trypan blue dye exclusion method.

2.8 Wound healing assay

The L929 cells were treated with 100 nM of CNP for 24 h and irradiated with UVA (30 J/cm^2). Immediately after irradiation, a sterile 200 μL pipette tip was used to make a straight scratch on the monolayer of cells attached. The pictures were taken at the time 0, 24 and 48 h after the scratch. Wound repopulation was assessed with a light microscope (Olympus BX51, Miami, FL, USA) equipped with a digital camera (Olympus C5060, Miami, FL, USA). Photomicrographs were taken at ×5 magnification and cell proliferation area was mesured using Image- J 1.45S software (Wayne Rasband, National Institutes of Health, Bethesda, MD, USA).

2.9 Senescence-associated β-galactosidase (SA-βG) assay

The senescence-associated b-galactosidase (SA-βG) was performed as preouvisly described [15]. The L929 cells were treated with 100 nM CNP for 24h or 100 μM NAC for 1 h. Next, the cells were irradiated with UVA (15 J/cm^2) for 3 consecutive days and incubated for 24h in a humidified incubator. Cells were washed in

phosphate-buffered saline (PBS; pH 7.4) and fixed for 5 min in 2% formaldehyde and 0.2% glutaraldehyde in PBS. After, 100 μL of staining solution (citrate–phosphate buffer with 100 mM potassium ferricyanide, 100 mM potassium ferrocyanide, 5 M NaCl, 0.2 M $MgCl_2$) was added followed by the addition of 10 μL of 2 mM Di-β-D-Galactopyranoside (FDG, Molecular Probes, Eugene, OR, USA) per well. The plate was incubated at 37 ºC in the dark for 24 h. After, the supernatant (100 μL) was transferred to a 96-black-well plate in triplicates for fluorescent measurement using a spectrofluorometer (Victor X3; PerkinElmer; λex = 485 nm, λem = 535 nm). doxorubicin (DOXO, 5 μg/mL), used as a positive control, was added to cells for 24 h followed by incubation of 3 days. The fluorescence precentage was expressed as arbitrary fluorescence units per μg of protein dertermined by Bradford method.

2.10 Cell death

Caspase-like activity was performed using an EnzChek Caspase-3 #1 Z-DEVD-AMC Substrate Assay Kit (Molecular Probes, Eugene, OR, USA). The L929 cells were treated with 100 nM CNP for 24h or 100 μM NAC for 1 h. Next, the cells were irradiated with UVA (30 J/cm^2). After, the cells were incubated for 24 h and after, collected, washed, resuspended in PBS buffer and processed according to the manufacturer's instructions. The samples were then added to a black 96-well plate, and fluorescence was measured in a spectrofluorometer (Victor X3; PerkinElmer; λex = 342 nm, λem = 441 nm). Camptothecin (CAMP, 100 μM, 1h treatment) was used as a positive control. An additional group was incubated with the caspase inhibitor Ac-DEVD-CHO. The fluorescence precentage was expressed as arbitrary fluorescence units per μg of protein dertermined by Bradford method.

2.11 Mitochondrial membrane potential (Δψm) measurement

We examined the mitochondrial membrane potential (Δψm) through tetramethyl rhodamine ethyl ester (TMRE, Molecular Probes, Eugene, OR, USA) labeling. In brief, L929 cells were treated with 100 nM CNP for 24 h or 100 μM NAC for 1 h and irradiated with UVA (30 J/cm^2) followed by 2h incubation. The cells were washed, harvested and resuspended in saline solution (0.9% sodium chloride solution), and 100 nM TMRE was added for 20 min in the dark at 37ºC [16]. After, cells were washed, and cell-associated fluorescence was detected using a spectrofluorimeter plate reader (VICTOR X3, PerkinElmer, USA, λex = 549 nm, λem = 575 nm). Carbonyl cyanide 3-chlorophenylhydrazone (CCCP, 200 μM, 1 h treatment – Sigma-Aldrich, St. Louis, MO, USA) was used as a positive control. The fluorescence precentage was expressed as arbitrary fluorescence units per μg of protein dertermined by Bradford method.

2.12 Western blot analysis

Western blot was performed to detect ERK 1/2 protein. After treatment with 100 nM CNP for 24h or 100 μM NAC for 1 h L929 cells were irradiated with UVA (30 J/cm^2) followed by 2 h incubation. Next, cellswere lysed in lysis buffer (1 %) and total protein (20 μg) was separated by 12% sodium dodecyl sulfate polyacrylamide gel electrophoresis and transferred to 0.22-μm nitrocellulose membranes. The membranes were blocked with 5% albumin diluted in a Tris-buffered saline solution containing 1% Tween-20 (TBST) and then incubated overnight at 4°C in solutions with primary antibodies (1: 50) against Erk1/2 (sc-514302), phospho ERK1/2 (sc-81492) or PCNA (1: 10000, sc-56) (Santa Cruz Biotechnology, Santa Cruz, CA, USA). The membranes were washed three times with TBST before an incubation for 1 h in solution with anti-mouse secondary antibody HRP-conjugated (1:10000) (Santa Cruz Biotechnology, Santa Cruz, CA, USA). Proteins were detected by western blotting luminol reagent (Santa Cruz Biotechnology, Santa Cruz, CA, USA) using CCD camera imaging system

(ImageQuant LAS 500, GE Healthcare Life Sciences, Uppsala, Sweden). Image- J 1.45S software (Wayne Rasband, National Institutes of Health, Bethesda, MD, USA). Quantitation of the relative amount of p-ERK 1/2 was normalized to the control PCNA.

2.13 Statistical Analysis

All other experiments were run in duplicate and repeated three times. The significant differences between mean values were expressed as mean ± standard deviation (SD), followed by analysis of variance (ANOVA) and Tukey test (Prism 5.0 software) to evaluate the significance of differences at the 5% level ($P<0.05$) of confidence.

3. Results

3.1 CNP synthesis and characterization

Indepth analysis the physiochemical characterization of CNP material has been already reported in our earlier published article [13]. Further here we continued with the detailed X-ray photoelectron spectroscopy (XPS) survey spectral lines of CNP in Figure 1 showing that these CNP products contains Ce, O and surface contaminated carbon as the primary elements. However, CNP survey spectral line shows the additional N1s which is ascribed to nitrate compound from Cerium nitrate hexahydrate precursor used for the CNP material synthesis. Figure 1b shows the Ce3d envelop from CNP material and spectra are fitted with 5 sets of spin-orbit split doublets of Ce 3d (3d5/2 and 3d3/2) with a Gaussian-Lorentzian peak shape after the subtraction of smart background in Avantage software. To ensure proper peak fitting, the area ratio of 3d spin-orbit split

doublets, their splits, well as peak positions were considered. In addition, spectra were analyzed using an automated incremental peak deconvolution program which varied the peak height within an envelope over a complete range to determine the best fit, checked by using the X-squared value to the actual data. With this method, the percent concentration of surface Ce^{3+} (or Ce^{4+}) ions in the film was calculated from the ratio of sum of the integrated areas of the XPS 3d peaks related to Ce^{3+} (or Ce^{4+}) to the total integral area for the whole Ce 3d region. The quantified concentration of Ce^{3+} in CNP materials was 58%. The lower surface Ce^{3+} concentration in CNP is also visible in the fitted Ce (3d) spectrum (Figure 1b). The peak position at ~916 eV corresponds to Ce^{4+} oxidation state. Thus, variation in this peak intensity, comparative to other peaks, provides quantifiable information with respect to the relative difference in concentration of each oxidation state. The relative intensity of the peak around 916 eV is significantly low for CNP.

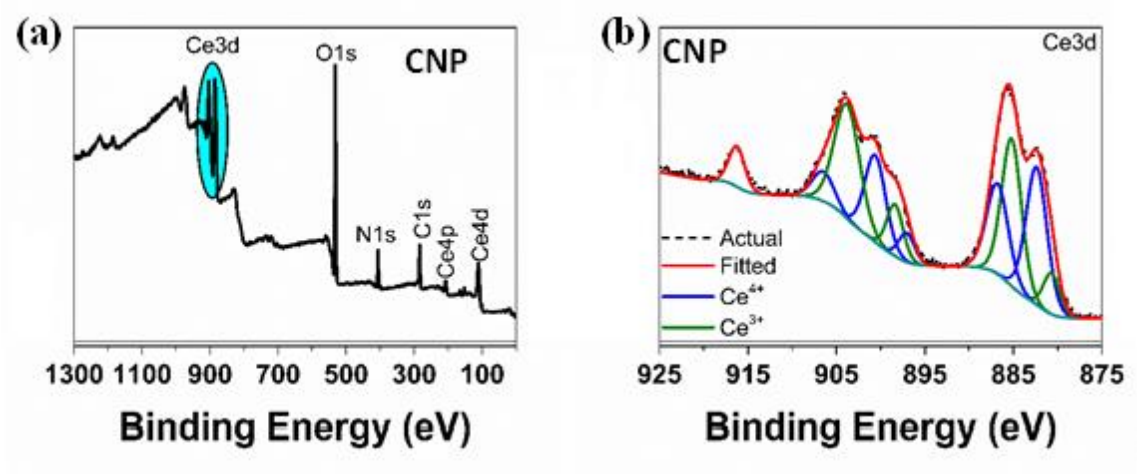

Figure 1: (a) XPS survey spectra of CNP (b) XPS peak fitted Ce3d spectra of CNP. Deconvoluted peaks in CNP show the mixed oxidation state of Ce^{3+} (green color) and Ce^{4+} (blue color).

Nanoceria is absorbed by L929 cells

To determine the efficiency of nanoceria uptake into L929 cells, cells were loaded with nanoceria conjugated with fluorescein isothiocyanate (CNP-FITC). The best time of uptake was observed when cells were treated for 24 h (Fig.2A and B). At 24 h the fluorescence significantly increased 3.1 fold compared with NC. At 1 and 2h of treatment, fluorescence incresead 1 and 1.4 fold, respectively, however this effect was not significant compared with control (NC).

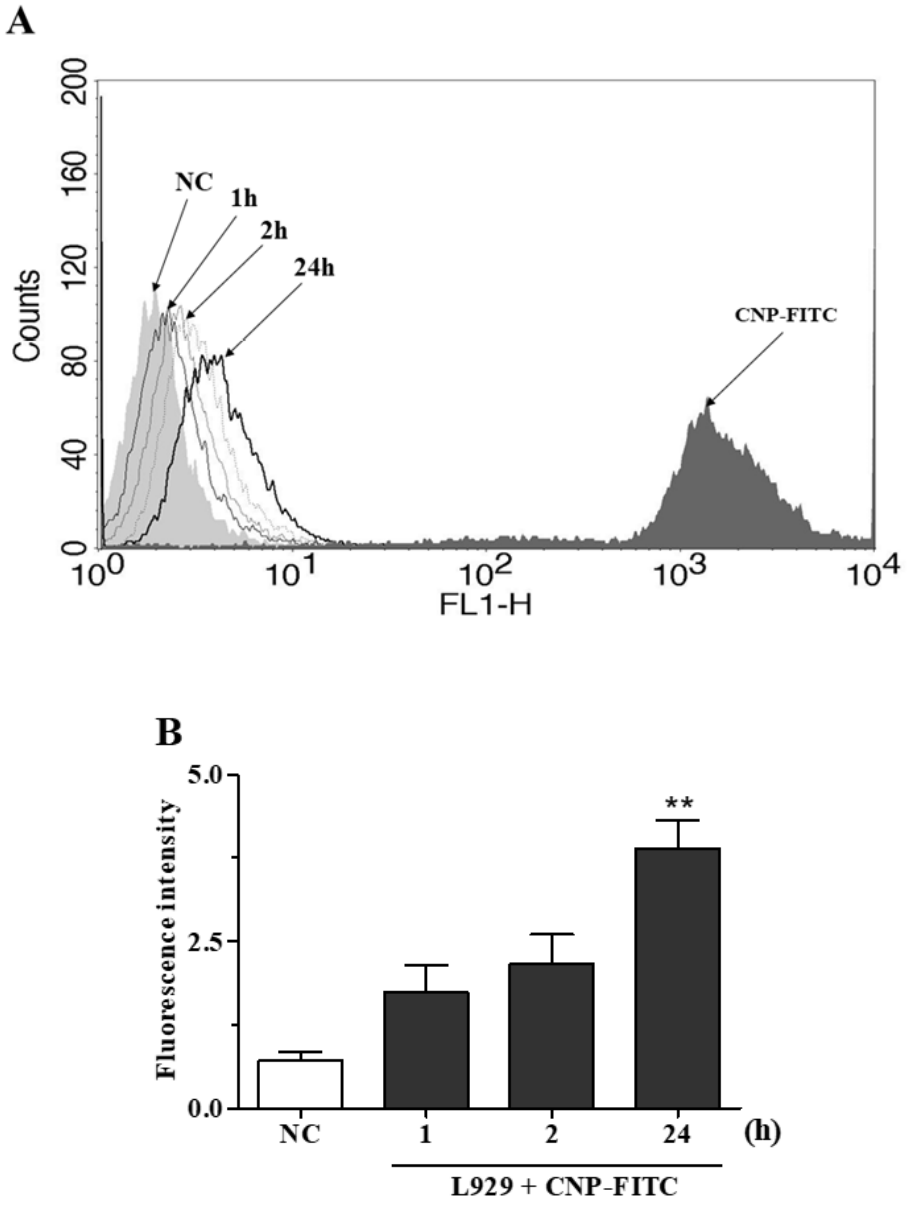

Figure 2. CNP uptake by L929 cells. (A) The histograms and (B) graphic bars show the fluorescence intensity of L929 cells treated (1, 2 and 24h) with CNP-FITC (100 nM) at different time points analyzed by FACS Calibur flow cytometer with 488 nm excitation. NC (non-treated cells), CNP-FITC (nanoceria conjugated with CNP with no cells). $^{**}p < 0.01$: significantly different from nonirradiated and nontreated cells (NC).

CNP has cytoprotective and photoprotective effect in UVA-irradiated L929 fibroblasts

Cell viability was assessed in fibroblast cell line L929 treated with CNP at diferente concentrations 500, 250, 100, 50, 10 and 5 nM using MTT assay. Figure 3A shows that CNP does not affect the viability of L929 cells compared with non-treated group (NC). Moreover, it was noted that 100 nM CNP significantly induces cell growth

(15%) compared with control (non-treated cells). The photoprotective effect of CNP in L929 cells against UVA radiation was also evaluated. As shown in Fig. 3B, after irradiation the cells treated with 100 nM CNP significantly increased (26%) cell viabilty compared with UVA group. Based on this, 100 nM was chosen to further investigations.

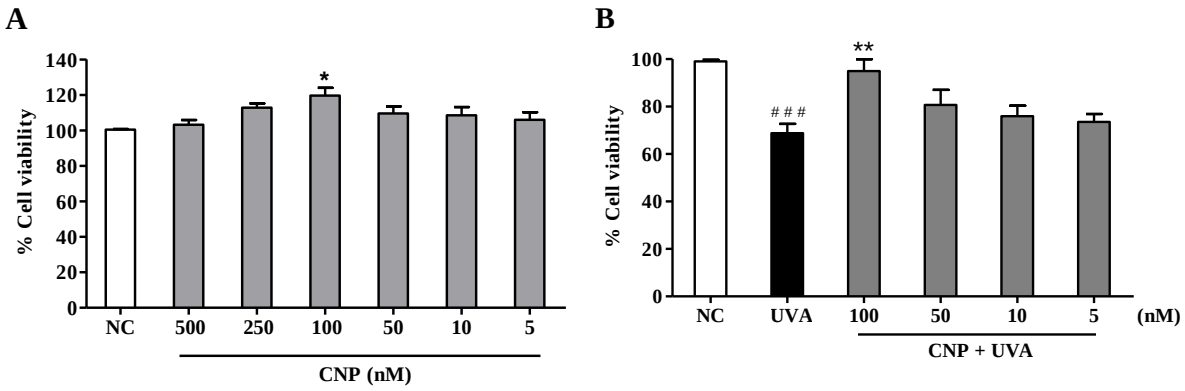

Figure 3**.** Effect of CNP on viability of non-irradiated and irrradiated L929 cells. (A) Cells were treated with CNP (500, 250, 100, 50, 25 and 5 nM) for 24 h. (B) Cells were treated with CNP (100 nM), exposed to UVA radiation (30 J/cm^2) and incubated for more 24 h. In both experiments, cell viability was assessed by MTT assay. NC (non–treated and non irradiated cells), CNP (treated and non-irradiated cells), UVA (non-treated and irradiated cells) and CNP + UVA (treated and irradiated cells). *p < 0.05: significantly different from NC, **p < 0.01: significantly different from UVA, $^{\#\#\#}p$ < 0.001: significantly different from NC.

CNP decreases ROS formation and increases SOD activity and GSH level in UVA-irradiated L929 fibroblasts

The intracellular antioxidant activity of nanoceria on UVA-induced L929 oxidative stress was analized using H_2DCF-DA. We observed that immediatelly after irradiation, CNP showed a great effect, reducing 60% of intracelular ROS formation, compared with UVA (Fig 4A). Similar effect (60%) was observed for SOD treatment (Fig. 4A). NAC and CAT inhibited 55% and 30% of ROS, respectively compared with UVA. A time course analysis (Fig. 4B) showed that CNP effect persisted for 48 h. After 1 h of a single dose of UVA radiation, CNP significantly (26%) reduced ROS formation

compared with UVA. This effect lasted until 24 h with significantly ROS reduction up to 30% compared with UVA. After an additional dose of UVA irradiation, CNP was still able to reduce ROS production. This effect was again persistent for more 24 h with a significantly ROS reduction up to 46 %. For the time 0, 26 and 48 h we can see that CNP decrease UVA-induced ROS production, however it was not significative.

CNP effect on L929 intracelular antioxidant enzymes SOD and GSH activity was also determined. Figure 4C and D show that the exposure of L929 cells to UVA significantly decreases SOD activity (55%) and GSH levels (50%) compared with NC. The treatment with CNP led to a significant increase in the activity of SOD (25%) and GSH levels (47%) compared with UVA. Pretreatment with NAC also significantly increased SOD activity and GSH levels by 25 and 65%, respectively.

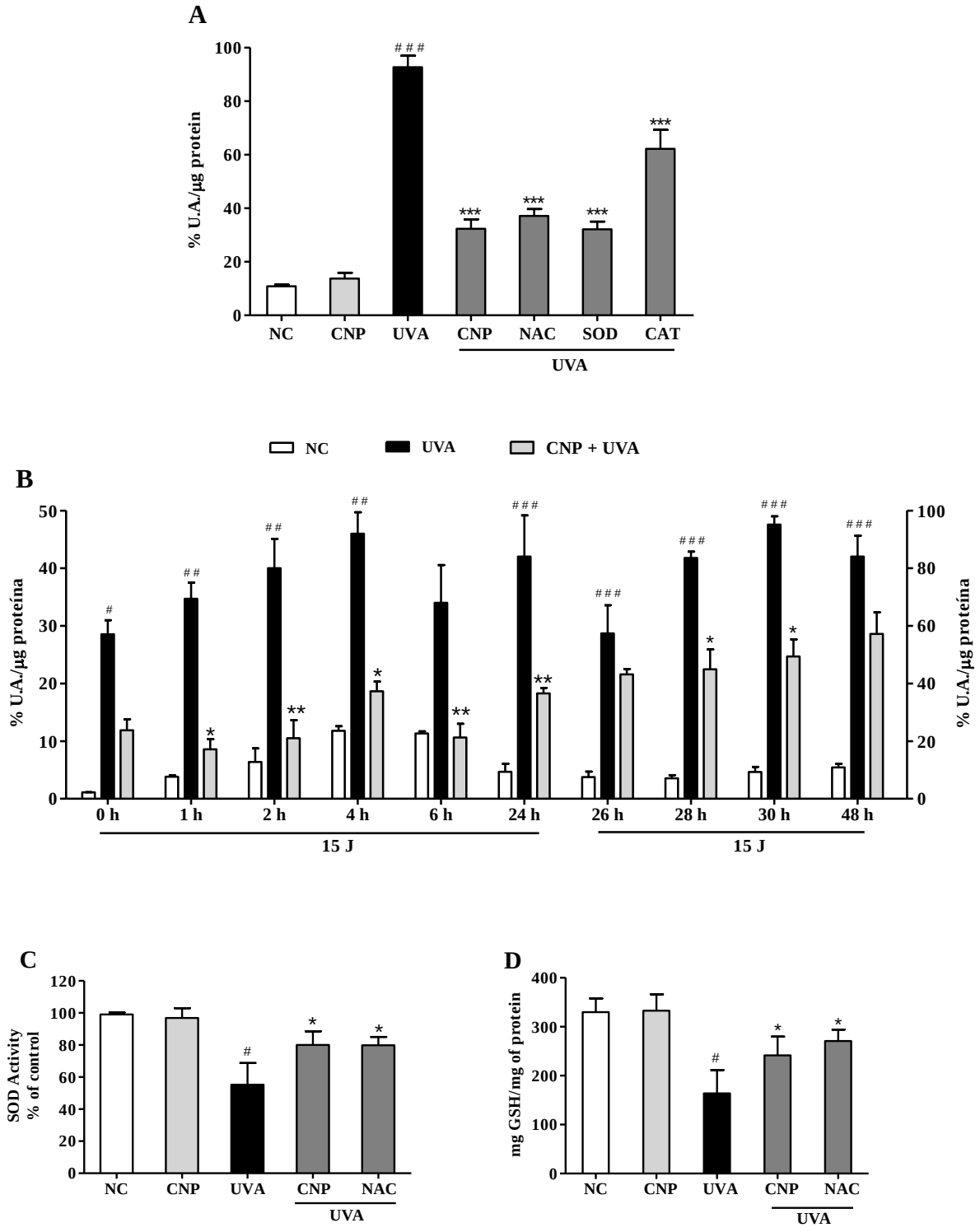

Figure 4. CNP antioxidant effect on UVA-irradiated L929 fibroblasts. (A and B): detection of total ROS in L929 cells treated with CNP (100 nM) for 24 h and irradiated with UVA, using H_2DCFDA. (A): cells were exposed to UVA radiation (30 J/cm^2) and the readings performed immediately after irradiation. (B): cells were exposed to UVA radiation (15 J/cm^2), and the readings performed in different times (0, 1, 2, 4, 6 and 24 h). After 24 h of incubation the cells were reirradiated with 15 J/cm^2 and the readings performed in different times (26, 28, 30 and 48 h). The level of intracellular ROS is expressed as the percentage mean of DCF fluorescence

intensity. (C) detection of SOD activity and (D) GSH levels in L929 cells treated with CNP (100 nM) for 24 h and irradiated with UVA (30 J/cm^2). The readings were performed after 1 h. SOD activity assessed by autoxidation of pyrogallol. GSH content was assayed by the o-phthalaldehyde method. NC (non-treated and non-irradiated cells), UVA (non-treated and irradiated cells), CNP + UVA (treated and irradiated cells), CNP (treated and non-irradiated cells), NAC + UVA (cells treated with N-Acetylcysteine and irradiated). SOD + UVA (cells treated with superoxide dismutase and irradiated), CAT + UVA (cells treated with catalase and irradiated). *p<0.05: significantly different from UVA, **p<0.01: significantly different from UVA, $^{\#\#\#}p$<0.001: significantly different from NC.

CNP induces L929 cell proliferation in UVA-irradiated L929 fibroblasts

To understand the possible ability of CNP on L929 cell proliferation, we performed a growth curve assay. In non-irradiated cells CNP increased significantly about 12% cell growth in all tested days compared with NC (Fig. 5A). CNP treatment also induced a progressive cell growth in 1, 2, 3, 4 and 5 days after radiation of 2.5, 5.1, 5.3, 11 and 15 fold, respectively compared with UVA (Fig 5A). Cells were also counted 24 h after irradiation considering live and dead cells. As shown in Fig. 5B, the dead cells in CNP irradiated cells was 22 % and 14% in NAC treated cells compared with UVA.

In addition of CNP induced L929 cell growth, we evaluated the CNP L929 regeneration potential in wound repair. Wound recover in cells under normal conditions (NC) was 44% at 24h and 58% at 48h compared with time zero (Fig. 5C and D). The wound repair was significantly higher in cells treated with CNP than those in the control group (NC). This increase was 64% and 81% after 24 h and 48 h, respectively. In UVA group was observed no proliferation of cells, but CNP treatment after UVA radiation promoted 30 and 55% of wound repair after 24 and 48 h of irradiation, respectively.

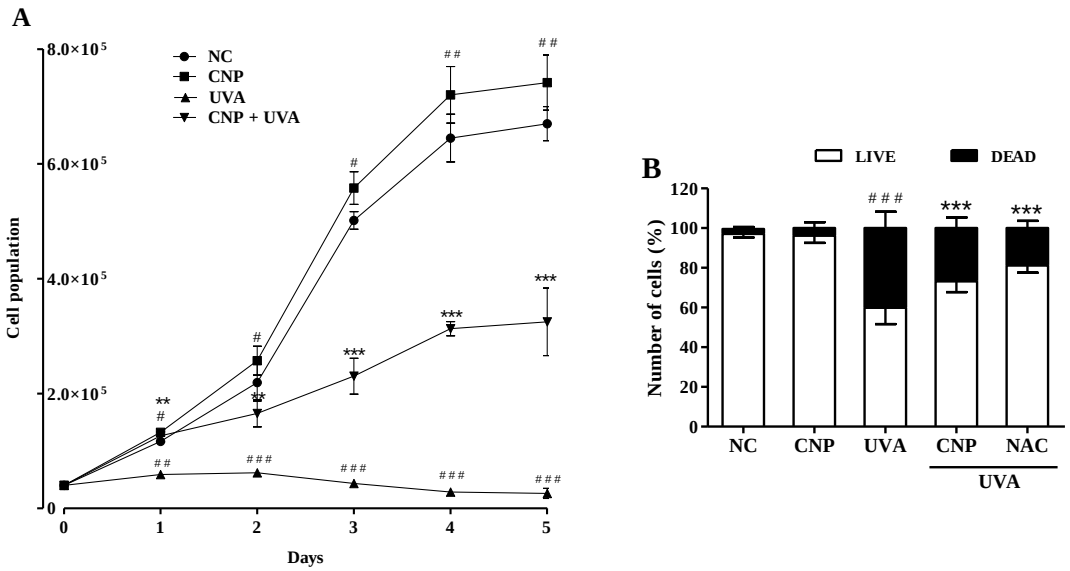
A
Cell population
8.0×10⁵
6.0×10⁵
4.0×10⁵
2.0×10⁵
0
NC
CNP
UVA
CNP + UVA
Days
0
1
2
3
4
5
B
LIVE
DEAD
Number of cells (%)
120
100
80
60
40
20
0
NC
CNP
UVA
CNP
NAC
UVA

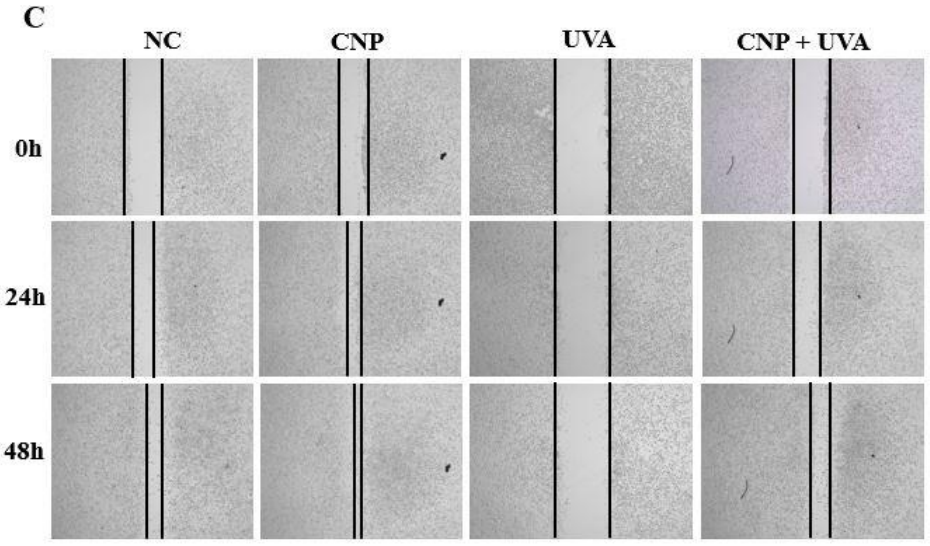
C
NC
CNP
UVA
CNP + UVA
0h
24h
48h

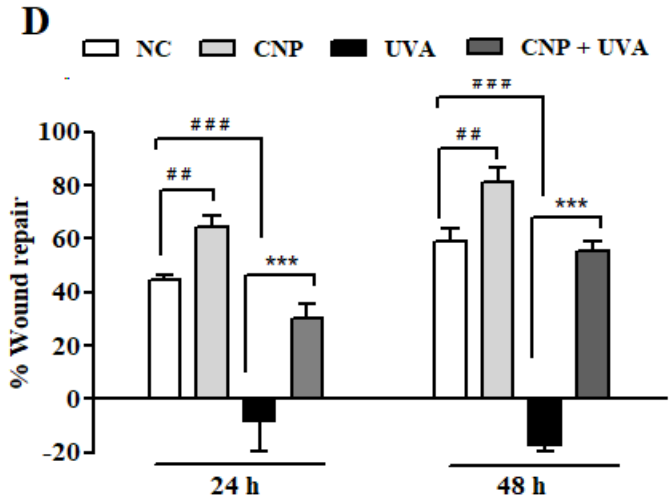
D
NC
CNP
UVA
CNP + UVA
% Wound repair
100
80
60
40
20
0
-20
24 h
48 h

Figure 5. Evaluation of L929 cell proliferation. (A, B) Effect of CNP on L929 cells growth. Cells were treated with CNP (100 nM) for 24 h followed by irradiation with UVA (30 J/cm^2) and incubated for 1, 2, 3, 4 and 5 days. Every 24 h cells were counted using trypan blue dye exclusion method, for 5 days considering live cells. Dead and live cells were quantified after 24h incubation after irradiation (day 1) and counted by trypan blue dye exclusion method. (C and D) Wound healing assay. L929 cells were treated with 100 nM CNP for 24 h, irradiated with 30 mJ/cm^2 UVA, and cells were scratched. Representative cell images from each group in the indicated time points after scratrch are shown. The area of the wound was measured at the 0, 24 and 48 h time points and compared in every group. Photomicrographs were taken at ×5 magnification in a light microscope. NC (non-treated and non-irradiated cells), UVA (non-treated and irradiated cells), CNP + UVA (treated and irradiated cells), CNP (treated and non-irradiated cells), NAC + UVA (cells treated with N-Acetylcysteine and irradiated). ## $p < 0.01$: significantly different from NC, ### $p < 0.001$: significantly different from NC, *** $p < 0.001$: significantly different from UVA.

CNP inhibits senescence and apoptosis in UVA-irradiated L929 fibroblasts

The effect of CNP in UVA-induced cellular senescence of L929 cells was also evaluated using fluorescein di-β-D-galactopyranoside (FDG). As shown in Fig. 6A, we observed that UVA radiation induced significantly cell senescence (66%) after three days of irradiation. β-galactosidase activity was not detected after a short period of analysis (less than 3 days after irradiation) (data not shown). CNP treatment significantly decreased (32%) β-galactosidase activity in irradiated cells, compared with UVA. A significant decrease in β-galactosidase activity was also observed for NAC (45%). DOXO, used as a positive control, increased 89% of β-galactosidase activity compared to NC.

The effect of CNP in UVA-induced apoptosis of L929 cells was assessed by measuring Caspase 3/7 levels. Figure 6B shows a significant increase in the activity of Caspase 3/7 (57%) in UVA irradiated L929 cells compared with NC. CNP treatment decreased by 25% the activity of Caspase 3/7 in irradiated cells, compared with UVA. For NAC this effect was higher (53%) than CNP. CAMP, used as a positive control, increased the activity of Caspase 3/7 like activity by 74%, compared with NC. As

expected, the group incubated with the caspase inhibitor Ac-DEVD-CHO decreased the UVA (43%) and CAMP (55%) effect in Caspase 3/7 activity. Interestingly, CNP had a similar effect (25%) as observed for the caspase inhibitor on UVA-induced Caspase 3/7 activity.

Additional signals of apoptotic features were assayed studing mitochondrial dysfuntion. Thus, the effect of CNP in mitochondrial membrane potential of UVA irradiated L929 cells was assessed using TMRE. Figure 6C shows significant mitochondrial membrane despolarization in UVA exposured cells (44%), compared with CN. CNP treatment protected cells by significantly decreasing 20% the mitochondria depolarization, compared with UVA. Similar effect was observed for NAC (26%).

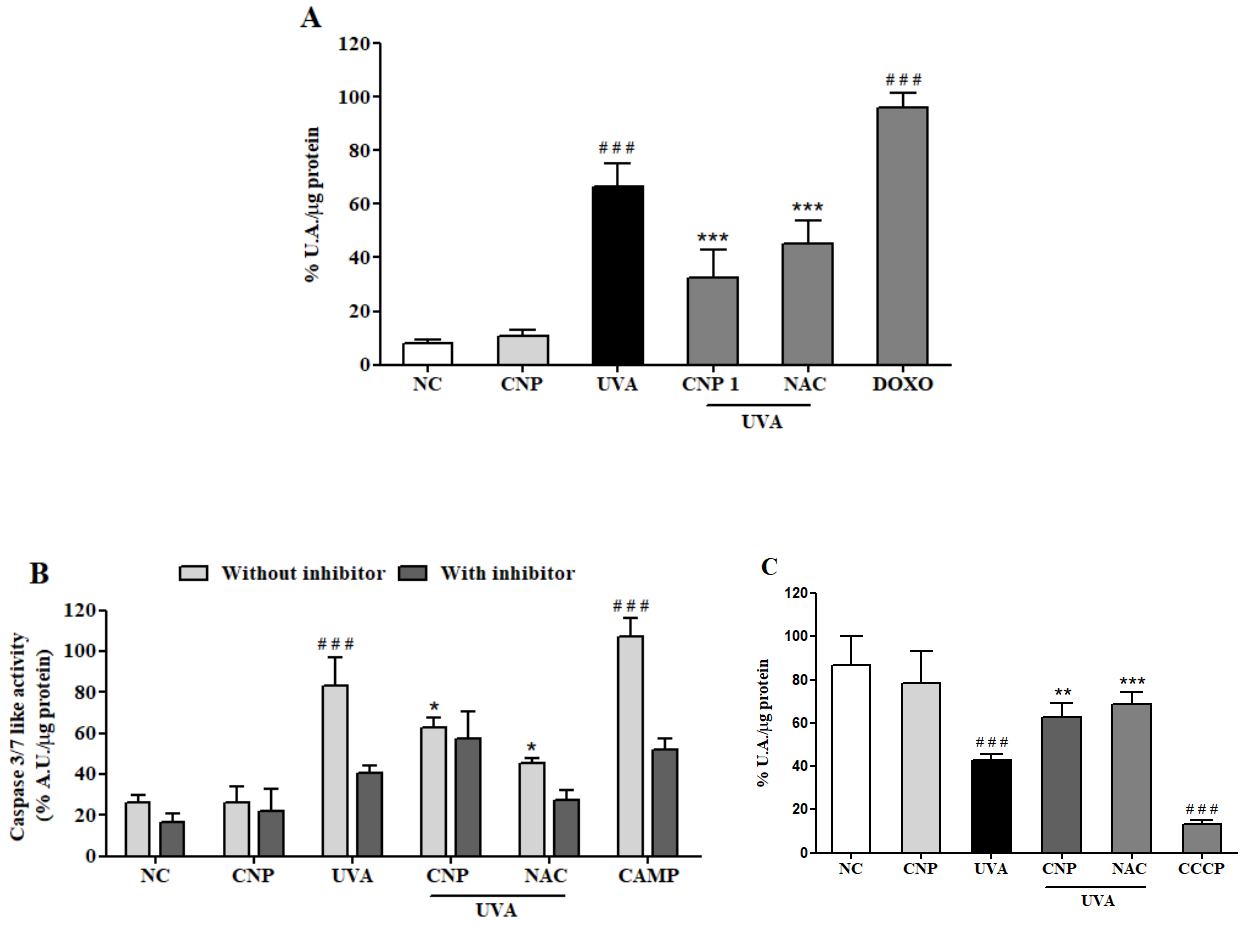

Figure 6. Assessment of senescence and cell death in L929 cells. (A) Senescence-associated b-galactosidase (SA-bG) activity measured based on fluorescein production. Cells were treated with 100 nM CNP and irradiated with to 10 J/cm^2 for 3 consecutive days and incubated for 24h. Fluorescence was measured after 24 h of incubation with FDG. (B) Caspases 3/7 like activity. Cells were treated with 100 nM CNP and irradiated with 30 mJ/cm^2 UVA. Caspase-3/7 activity was measured using Z-DEVD-AMC substrate after 24 h of irradiation. (C) Measurement of mitochondrial dysfunction. Cells were treated with 100 nM CNP and irradiated with (30 J/cm^2) After 2 h of incubation, cells were stained with the fluorescent probe (TMRE, 100 nM). NC (non-treated and non-irradiated cells), UVA (non-treated and irradiated cells), CNP + UVA (treated and irradiated cells), CNP (treated and non-irradiated cells), NAC + UVA (cells treated with N-Acetylcysteine and irradiated), DOXO (cells treated with doxorubicin and non-irradiated), CAMP (cells treated with camptothecin and non-irradiated), CCCP (cells treated with carbonyl cyanide 3-chlorophenylhydrazone and non irradiated. ### $p < 0.001$: significantly different from NC, *** $p < 0.001$: significantly different from UVA, ** $p < 0.01$: significantly different from UVA, * $p < 0.05$: significantly different from UVA.

CNP inhibits ERK phosphorylation in UVA-irradiated L929 fibroblasts

To assess ERK contribuition on death, survival or proliferation of L929 cells under UVA radiation we performed western blot assay. As shown in Fig. 7A and B, ERK phosphorylation in UVA group was significantly increased after 2 h (1.31 fold), 12 h (1.98 fold) and 24 h (2.87 fold) of irradiation compared with NC. In CNP treated cells ERK phosphorylation was significantly lower in 12 h (1.79 fold) and 24h (2.2 fold) compared with UVA group. NAC used as an antioxidant control decreased UVA-induced ERK phosphorylation in 12 h (1.4 fold) and 24 h (1.21 fold) but this decrease was not significant.

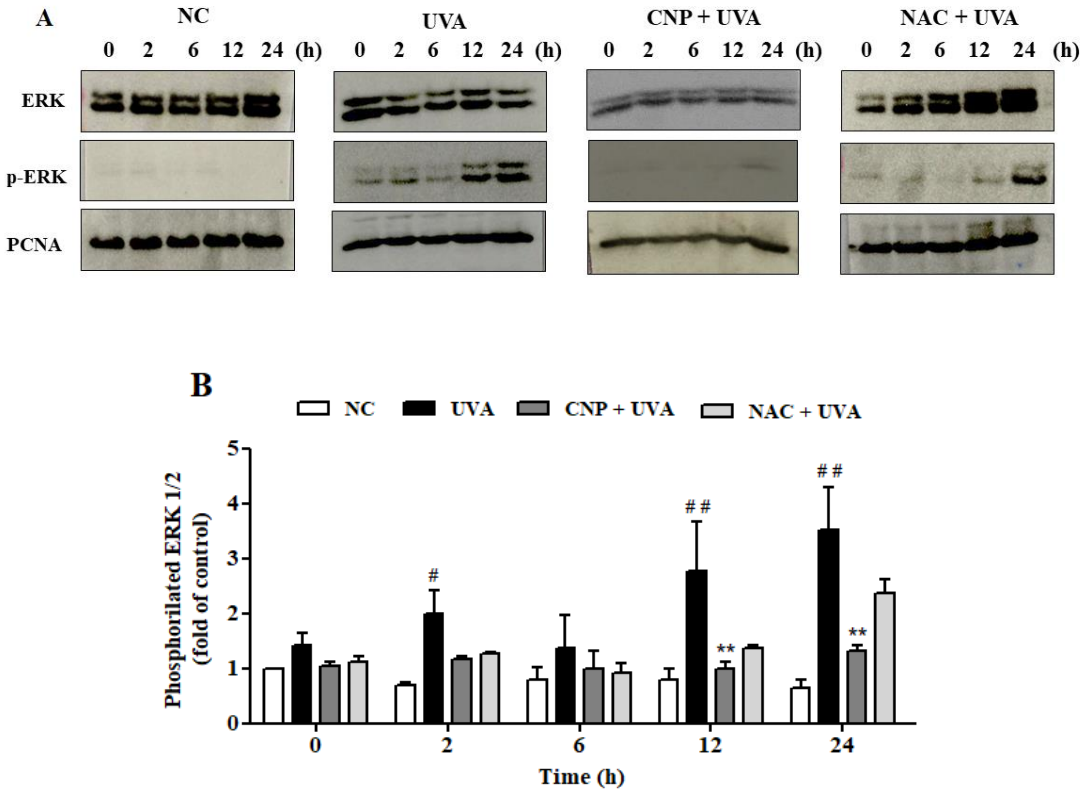

Figure 7. ERK phosphorylation and cell cycle analysis. (A and B) ERK 1/2 phosphorylation was performed by Western blot. After 24 h of CNP (100nM) treatment and UVA exposure (30 J/cm^2) cell lysates were prepared for subsequent analysis by polyacrylamide gel electrophoresis followed by western blot analysis for ERK 1/2 (ERK total), phospho-ERK 1/2 (p-ERK 1/2) and PCNA. The density of each band was normalized with corresponding PCNA levels (bar graphs). NC (non-treated and non-irradiated cells), UVA (non-treated and irradiated cells), CNP + UVA (treated and irradiated cells), CNP (treated and non-irradiated cells), NAC+UVA (cells treated with N-Acetylcysteine and irradiated). # $p < 0.05$: significantly different from NC, ** $p < 0.01$: significantly different from UVA, # # $p < 0.01$: significantly different from NC.

4. Discussion

CNPs cytoprotective effect was already described in UVA-irradiated fibroblasts [17]. This effect is closed related to CNPs' self-regenerative redox cycling property combining CAT- and SOD-mimetic antioxidant activities [5,6]. Here our goal was to reveal whether under UVA-induced oxidative redox imbalance CNP might also induce fibroblasts proliferation instead only protection. Our data showed that CNP restores the endogenous antioxidant enzymes activity which in turn prevents cell aging and triggers the activation of signaling pathways that control cell proliferation.

We first showed that CNP induced no L929 cytotoxicity even at high concentrations (data not shown). We also observed that nanoceria uptake by L929 cells was time dependent and at 24 hours it had a significant uptake and seemed to be located around the nucleus. Uptake efficiency is affected by particle properties, experimental conditions and cell type [18]. Co-localizion with these CNPs has already been reported and showed its localization in multiple compartments such as mitochondria, lysosomes and endoplasmic reticulum and in the cytoplasm and the nucleus [19].

The UVA radiation might induce cellular damage through the activation of ROS overproduction [20]. Our results showed that the pre treatment with nanoceria was effective to protect L929 cells from the toxic effect of UVA and decrease L929 cells UVA-induced ROS production after 24 h of UVA irradiation and this effect persist even after a further dose of UVA exposure.From this data we could see that UVA-irradiated fibroblasts has increased ROS production in a time dependent manner and nanoceria was still active up to 48h. This extended ROS inhibition effect of nanoceria is mainly centered on Cerium that can exist in both valence state (Ce^{3+}/Ce^{4+}) and in the presence of oxygen is able to interchange between these two valences. This interchangeability of nanoceria also allows its self-regeneration, which may collaborate to its extended activity as well. Higher concentration of Ce^{3+} on the nanoparticle surface also means SOD like activity as it sequester O_2^- by reducing to Ce^{4+}. In addition, nanoceria restored important antioxidant enzymes, SOD and GSH. These effects were possible due to CNP enzimes like activities and also due to decrease of ROS and consequent attenuation of oxidative stress, which was also observed with the well-known antioxidant NAC.

We then found that the CNP antioxidant protection against UVA irradiation also mediate intracellular ROS-dependent signaling pathways that are regulated by low ROS concentration. Pretreatment with nanoceria as well as NAC significantly decrease UVA-induced cellular senescence. ROS play a central role as mediators of cellular senescence

leading to permanet cell cycle G1 arrest [21,22]. Additionally, we found that nanoceria decreased apoptosis assessed by caspase3/7 levels and improve mitochondria ΔΨm by TMRE labeling. We also found that nanoceria not only inhibited L929 death but also induced L929 proliferation. Our data showed that nanoceria increased, in a time dependent manner, the proliferation in both non-irradiated and UVA-irradiated cells.

Nanoceria also showed to be able to stimulate wound regeneration even after irradiation. Some studies has also shown that the regenerative potential of cerium oxide nanoparticles in both cell culture and animal models [3,23,24]. The mechanism by which nanoceria induce cell proliferation is not completely understood. Some authors relate this effect to the valence state, others to activation of survival pathways such as stimulation of Bcl-2 expression and reduction of stress condition [25] or by nanoceria capacity in reducing apoptosis and activating ERK pathway [26]. Interestingly, herein we found that nanoceria increase proliferation however decreased UVA-induced ERK activation. The ERK activation is tighed regulated and its correlation with profiferation or cell death might depend on different factors such as the stimuli and cell type [26].

5. Conclusion

The direct antioxidant protective effect of nanoceria against the UVA-induced L929 damage play a key role in the activation of signaling pathways that control cell aging, death and proliferation. Nanoceria might be a potential ally with the intracellular antioxidant enzymes to fight UVA-induced photodamage and consequently drive cells to survival and proliferate mechanisms.

Acknowledgements

The authors gratefully acknowledge the reserach group from the Nanoscience Technology Center from University of Central Florida, Orlando, FL, US. We also gratefully thank Dr. Soumen Das for his assistance provided with this study.

This study was supported by grants from the Coordenação de Aperfeiçoamento de Pessoal de Nível Superior - Brasil (CAPES) – (Finance Code 001); COMCAP-UEM (Complex of Research Support Centers), Conselho Nacional de Desenvolvimento Científico e Tecnológico, PRONEX/Fundação Araucária and Financiadora de Estudos e Projetos.

References

[1] S. Singh, Nanomaterials Exhibiting Enzyme-Like Properties (Nanozymes): Current Advances and Future Perspectives, (2019). doi:10.1039/c8cs00457a.

[2] Q. Wang, H. Wei, Z. Zhang, E. Wang, S. Dong, Nanozyme: an emerging alternative to natural enzyme for biosensing and immunoassay, Trends Anal. Chem. (2018). doi:10.1016/j.trac.2018.05.012.

[3] S. Chigurupati, M.R. Mughal, E. Okun, S. Das, A. Kumar, M. Mccaffery, S. Seal, M.P. Mattson, Effects of cerium oxide nanoparticles on the growth of keratinocytes , fi broblasts and vascular endothelial cells in cutaneous wound healing, Biomaterials. (2012) 1–8. doi:10.1016/j.biomaterials.2012.11.061.

[4] S. Das, S. Chigurupati, J. Dowding, P. Munusamy, D.R. Baer, J.F. Mcginnis, M.P. Mattson, W. Self, S. Seal, Therapeutic potential of nanoceria in regenerative medicine Therapeutic potential of nanoceria in regenerative medicine, (2015). doi:10.1557/mrs.2014.221.

[5] E.T. and L.G. Ivana Celardo, Jens Z. Pedersen, Pharmacological potential of cerium oxide nanoparticles, (2011) 1411–1420. doi:10.1039/c0nr00875c.

[6] S. Singh, T. Dosani, A.S. Karakoti, A. Kumar, S. Seal, W.T. Self, A phosphate-dependent shift in redox state of cerium oxide nanoparticles and its effects on catalytic properties, Biomaterials. 32 (2011) 6745–6753. doi:10.1016/j.biomaterials.2011.05.073.

[7] M. Rinnerthaler, J. Bischof, M. Streubel, A. Trost, K. Richter, Oxidative Stress

in Aging Human Skin, Biomolecules. 5 (2015) 545–589. doi:10.3390/biom5020545.

[8] J. Krutmann, P. Schroeder, Role of Mitochondria in Photoaging of Human Skin : The Defective Powerhouse Model, J. Investig. Dermatology Symp. Proc. 14 (2009) 44–49. doi:10.1038/jidsymp.2009.1.

[9] P. Bainbridge, W. Healing, T. Repair, Wound healing and the role of fibroblasts, (2013).

[10] J. Chen, D. Jiao, M. Zhang, S. Zhong, T. Zhang, X. Ren, G. Ren, Concentrated Growth Factors Can Inhibit Photoaging Damage Induced by Ultraviolet A (UVA) on the Human Dermal Fibroblasts In Vitro, (2019) 3739–3749. doi:10.12659/MSM.913967.

[11] X. Liu, R. Zhang, H. Shi, X. Li, Y. Li, A. Taha, C. Xu, Protective effect of curcumin against ultraviolet A irradiation ‐ induced photoaging in human dermal fibroblasts, (2018) 7227–7237. doi:10.3892/mmr.2018.8791.

[12] E. Heather, D.S. Foster, M.T. Longaker, Fibroblasts and wound healing : an update, 13 (2018) 491–495.

[13] G. Pulido-reyes, I. Rodea-palomares, S. Das, T.S. Sakthivel, Untangling the biological effects of cerium oxide nanoparticles : the role of surface valence states, Nat. Publ. Gr. (n.d.) 1–14. doi:10.1038/srep15613.

[14] S. Schaffer, J. Gruber, L.F. Ng, S. Fong, Y.T. Wong, S.Y. Tang, B. Halliwell, The effect of dichloroacetate on health- and lifespan in C . elegans, (2011) 195–209. doi:10.1007/s10522-010-9310-7.

[15] N. Yang, M. Hu, A fluorimetric method using fluorescein di- b - D - galactopyranoside for quantifying the senescence-associated b -galactosidase activity in human foreskin fibroblast Hs68 cells, 325 (2004) 337–343. doi:10.1016/j.ab.2003.11.012.

[16] L. Xuan, J. Shi, C. Yao, J. Bai, F. Qu, J. Zhang, Q. Hou, Vam3 , a resveratrol dimer , inhibits cigarette smoke- induced cell apoptosis in lungs by improving mitochondrial function, Nat. Publ. Gr. 35 (2014) 779–791. doi:10.1038/aps.2014.17.

[17] Y. Li, X. Hou, C. Yang, Y. Pang, X. Li, G. Jiang, Photoprotection of Cerium Oxide Nanoparticles against UVA radiation-induced Senescence of Human Skin

Fibroblasts due to their Antioxidant Properties, Sci. Rep. (2019) 1–10. doi:10.1038/s41598-019-39486-7.

[18] V.A.N.D.E.M. Eent, A.N.V.A.N.W. Ezel, A.J. An, Critical Review CELLULAR UPTAKE OF NANOPARTICLES AS DETERMINED BY PARTICLE PROPERTIES , EXPERIMENTAL CONDITIONS , AND CELL TYPE, 33 (2014) 481–492. doi:10.1002/etc.2470.

[19] S. Singh, A. Kumar, A. Karakoti, W.T. Self, Unveiling the mechanism of uptake and sub-cellular distribution of cerium oxide nanoparticles w, (2010) 1813–1820. doi:10.1039/c0mb00014k.

[20] A. Valencia, I.E. Kochevar, Nox1-Based NADPH Oxidase Is the Major Source of UVA-Induced Reactive Oxygen Species in Human Keratinocytes, 128 (2008). doi:10.1038/sj.jid.5700960.

[21] A. Hernandez-segura, J. Nehme, M. Demaria, Hallmarks of Cellular Senescence, Trends Cell Biol. 28 (2018) 436–453. doi:10.1016/j.tcb.2018.02.001.

[22] R. Colavitti, T. Finkel, Critical Review Reactive Oxygen Species as Mediators of Cellular Senescence, 57 (2005) 277–281. doi:10.1080/15216540500091890.

[23] S. Chigurupati, M.R. Mughal, E. Okun, S. Das, NIH Public Access, 34 (2014) 2194–2201. doi:10.1016/j.biomaterials.2012.11.061.Effects.

[24] R. Davan, R.G.S. V Prasad, V.S. Jakka, R.S.L. Aparna, A.R. Phani, B. Jacob, P.C. Salins, D.B. Raju, Cerium Oxide Nanoparticles Promotes Wound Healing Activity in In-Vivo Animal Model Delivered by Ingenta to :, (2012). doi:10.1166/jbns.2012.1074.

[25] M. Bizanek, T.J. Webster, A.K. Roy, Increased viability of fibroblasts when pretreated with ceria nanoparticles during serum deprivation, (2018) 895–901.

[26] Y. Mebratu, Y. Tesfaigzi, How ERK1/2 activation controls cell proliferation and cell death is subcellular localization the answer?, Cell Cycle. 8 (2009) 1168–1175. doi:10.4161/cc.8.8.8147.